

Supplementary Materials of the paper “A new many-objective evolutionary algorithm based on generalized Pareto dominance”

Shuwei Zhu, *Student Member, IEEE*, Lihong Xu, *Senior Member, IEEE*, Erik D. Goodman and Zhichao Lu, *Student Member, IEEE*

I. SUMMARY OF RELATED WORK

Table S-I: Summary of recent proposed notable MaOEAs since the year of 2017.

II. DESCRIPTION OF SOME EXISTING MODIFIED PARETO-DOMINANCE AND NON-PARETO-DOMINANCE METHODS

In the paper, we compare (M -1)-GPD with modified Pareto dominance methods, like Cone ϵ -dominance [41], CDAS-dominance [42] and its adaptive version S-CDAS [43], CN α -dominance [44], GPO [45] and the non-Pareto-dominance method SDR [36].

- Cone ϵ -dominance

It can be seen as a hybridization of the concepts of ϵ -dominance [46] and of proper efficiency with respect to cones. Cone ϵ -dominance introduces a parameter k ($k \in [0, 1]$), and k is applied to control the shape of dominance area of a solution. When $k \rightarrow 0$, the cone ϵ -dominance is consistent with the traditional Pareto-dominance. When $k > 0$, the shape of the dominance area is a cone.

As for two solutions \mathbf{x} and \mathbf{y} , \mathbf{x} cone ϵ -dominates \mathbf{y} (denoted as $\mathbf{x} \prec_{cone\epsilon} \mathbf{y}$) if the following condition holds:

$$(\mathbf{x} \prec \mathbf{y}) \vee (\Psi \lambda = z | \lambda_i \geq 0, \forall i \in \{1, 2, \dots, M\}) \quad (10)$$

where Ψ is the cone ϵ -dominance matrix, $z = q - [p - \epsilon]$, and $\epsilon_i > 0$.

However, to improve the performance of an algorithm, except for the parameter ϵ that used for the ϵ -dominance, the cone ϵ -dominance has to add another parameter k into the algorithm. This parameter, together with ϵ , can limit the application of the algorithm.

- CDAS-dominance

First, CDAS is a representative relaxed dominance relation, which expands the dominance area of a candidate solution \mathbf{x} by modifying the objective values:

$$f'_i(\mathbf{x}) = \frac{\|f(\mathbf{x})\| \sin(\omega_i + S \cdot \pi)}{\sin(S \cdot \pi)} \quad (11)$$

where $f'_i(\mathbf{x})$ denotes the i -th objective value of \mathbf{x} after modification, $\|\cdot\|$ denotes the L_2 -norm, ω_i denotes the declination angle between \mathbf{x} and the i -th axis, and $S \in [0.25, 0.5]$ is a parameter for controlling the expanding degree.

In order to eliminate the parameter S , an adaptive version of CDAS, called self-CDAS (S-CDAS), was proposed [43]. The S-CDAS adaptively determines the expanding degree of a candidate solution \mathbf{x} according to the extreme solutions in the population:

$$f'_i(\mathbf{x}) = \frac{\|f(\mathbf{x})\| \sin(\omega_i + \phi_i)}{\sin(\phi_i)} \quad (12)$$

where $\phi_i = \arcsin \frac{\|f(\mathbf{x})\| \cdot \sin(\omega_i)}{\|f(\mathbf{x}) - p_i\|}$, and p_i is the extreme solution with respect to the i -th axis in the population. Note that, an obvious difference between S-CDAS and CDAS is that the boundary of the dominance area of \mathbf{x} in the sense of S-CDAS always intersects (but does not dominate) the extreme solutions.

- CN α -dominance

Recently, a new dominance, called CN α -dominance, combining the advantages of two existing dominance methods—i.e. α -dominance and CN-dominance—has been proposed [44]. The detail is as follows:

First, let $F'(\mathbf{x}) = (f'_1(\mathbf{x}), \dots, f'_M(\mathbf{x}))$, where

$$f'_i(\mathbf{x}) = f_i(\mathbf{x}) + \sum_{j \neq i}^M \alpha_{ij} f_j(\mathbf{x}) \quad (13)$$

To be specific, each objective in many-objective optimization is assumed to be equally important, and thus, for a given solution \mathbf{x} , it is reasonable to take all parameters α_{ij} ($i \neq j$) the same value (say, α). The parameter α at generation t is adjusted as: $\alpha(t) = \alpha_{\max} - t(\alpha_{\max} - \alpha_{\min})/G_{\max}$, where α_{\max} and α_{\min} are the lower bound and upper bound of α , and G_{\max} is the maximum generation.

Then, the final objective vector is defined by $\hat{F}(\mathbf{x}) = (\hat{f}_1(\mathbf{x}), \dots, \hat{f}_M(\mathbf{x}))$, where

$$\hat{f}_i(\mathbf{x}) = r(\max(\sin(\omega_i), \cos(\omega_i)))^H \quad (14)$$

where $r = \|F'(\mathbf{x})\|$, $\cos(\omega_i) = \frac{f'_i(\mathbf{x})}{r}$, $\sin(\omega_i) = \frac{\sqrt{\sum_{j \neq i} f'_j(\mathbf{x})^2}}{r}$, $0 < H \leqslant 1$.

Finally, the CN α -dominance can be defined as follows:

Definition 3 (CN α -dominance): A solution \mathbf{x} is said to CN α -dominate solution \mathbf{y} , denoted as $\mathbf{x} \prec^{CN\alpha} \mathbf{y}$, if and only if

$$\begin{cases} \forall i \in \{1, 2, \dots, M\} : \hat{f}_i(\mathbf{x}) \leq \hat{f}_i(\mathbf{y}) \\ \exists j \in \{1, 2, \dots, M\} : \hat{f}_j(\mathbf{x}) < \hat{f}_j(\mathbf{y}) \end{cases} \quad (15)$$

TABLE S-I
SUMMARY OF RECENT PROPOSED NOTABLE MAOEAS SINCE THE YEAR OF 2017

Algorithm	Characteristic
Decomposition-based	
g-DBEA [1]	It is the enhanced version of I-DBEA [2] with adaptive reference vectors.
MaOEDA-IR [3]	The regularity-based EDA model is proposed to generate favorable solutions and the dimension reduction is employed in the decision space to speed up the estimation search. Uniformly distributed reference vectors are used to maintain population diversity.
MOEA/D-2ADV [4]	Search along the boundary direction vectors to achieve fast convergence at first; then delete poor reference vectors, add new ones.
MOEA/D-LWS [5]	A localized weighted sum approach is proposed to solve nonconvex problems, but it still faces problems with maintenance of diversity.
MOEA/D-SOM [6]	Weight design for decomposition-based MaOEAs using the self-organizing map (SOM).
MOEA/D-AM2M [7]	An adaptive region decomposition and weight vectors design are employed to extract useful information from the evolving population.
MOEA/AD [8]	Two populations are coevolved by two subproblem formulations with different contours and adversarial search directions.
MaOEA-IT [9]	Convergence and diversity are addressed in two independent and sequential stages, then the learned reference lines are used to preserve diversity.
PAEA [10]	Simultaneously using adaptive search directions and two reference points (the ideal and nadir points), and an angle-based elimination procedure is adopted to maintain diversified solutions.
CPSO [11]	Coevolve multiple swarms and develop a bottleneck objective learning strategy to accelerate convergence rate. The reference-point-based environmental selection of NSGA-III is directly used for preserving diversity.
B-NSGA-III [12]	In addition to emphasizing extreme objective-wise solutions, it also tries to find solutions near intermediate undiscovered regions of PF.
ASEA [†] [13]	Develop the two-stage sorting scheme (i.e. convergence-then-diversity-based sorting) based on the idea of decomposition. It measures the convergence by weighted sum, and measures the diversity by the acute angle to the reference directions.
DDEA [14]	Dynamical decomposition is proposed using the solutions themselves as the reference points instead of predefined weights.
CLIA [15]	It adopts two interacting processes, i.e., the cascade clustering and the reference point incremental learning, for evolving population.
MP-DEA [16]	Approximate irregular PFs using a set of well-distributed NBI (Normal-Boundary Intersection) directions.
DrEA [17]	It applies the customized decomposition-based dominance relationship with adaptive strategy to each subpopulation of the M2M framework [18].
hpaEA [19]	Hyperplane in local region is used to identify prominent solutions and enhance selection pressure, and reference weights are used for diversity.
DECLA [20]	Two new aggregation functions with distinct characteristics are designed to enhance the population diversity and accelerate the convergence.
ar-MOEA [21]	The ar-dominance relation combines angle preference and r-dominance to obtain a stricter partial ordering between non-dominated Pareto solutions.
Indicator-based	
1by1EA [22]	Design a convergence indicator in terms of the sum of objectives, and a distribution indicator de-emphasizing solutions that are too close to selected ones for the environmental selection.
AR-MOEA [‡] [23]	Develop an enhanced IGD indicator (i.e., IGD-NS) with reference point adaptation for better versatility.
NMPSO [24]	Both convergence distance and diversity distance are considered in the balanceable fitness estimation (BFE) approach.
MaOEA/IGD [‡] [25]	The IGD indicator is employed in each generation to select the solutions with favorable convergence and diversity.
I_{SDE}^+ [26]	It is a combination of sum of objectives and shift-based density estimation (SDE) [27].
GFM-MOEA [28]	The generic front modeling (GFM) is built to approximate the PF, then an indicator is defined based on the GFM.
2REA [29]	Distribution indicator is calculated based on the proposed adaptive position transformation (APT) distance to estimate the neighborhood density, while convergence indicator of each solution is measured using the sum of each objective.
R2HCA-EMOA [‡] [30]	Use the R2 indicator variant to approximate the HV contribution.
MaOEA-IBP [31]	A worst elimination mechanism based on the I_ϵ^+ indicator and boundary protection strategy is devised to enhance the balance of population convergence, diversity, and coverage
PMEA [32] [‡]	A polar-metric (p-metric)-based EA which adopts a set of uniformly distributed direction vectors. A modification is proposed to adjust the direction vectors of p-metric dynamically.
Others	
VaEA [33]	The maximum-vector-angle-first principle is used to guarantee the wideness and uniformity of the solution set. In the worse-elimination principle, worse solutions in terms of the convergence (measured by the sum of objectives) are conditionally replaced by other individuals.
MaPSO [34]	Add extreme solutions first and subsequently add the solutions with better convergence; then, use one-by-one remove to improve diversity.
MaOEA/C [†] [35]	Two clustering methods are used to maintain diversity and the sum of objectives is used as the indicator for convergence.
NSGA-II/SDR [†] [36]	Balances the convergence and diversity by adopting a tailored niching technique and the indicator in terms sum of objectives.
MDEA [†] [37]	The normalized minkowski distance to the ideal point is used for convergence, and max-min Euclidean distance is used for diversity.
MOPSO/DD [38]	The dominant difference of a solution is used to enhance selection pressure and L_p -norm-based density estimator makes it have good diversity.
PaRP/EA [39]	A global hyperplane is used to distinguish solutions of better convergence, distance based subset selection is used for diversity.
MaOES [40]	The maximum extension distance strategy is developed to guide individuals to keep uniform distance and extension to approximate the entire PF.

[†] They can be also regarded as partial indicator-based methods, due to the usage of the convergence indicator in terms of the sum of objectives (or the sum of distances to the ideal point).

[‡] They can be regarded as partial decomposition-based methods, since the IGD-type indicators are computed with reference points.

In the CN α -dominance, the Eq. (13) (i.e., α -dominance [47]) is used firstly to expand the dominated area for each solution, then based on the expanded area, use Eq. (14) (i.e. CN-dominance [48]) to further expand the dominated area. It can be seen intuitively from Fig. 4d that the CN α -dominated area by a solutions is larger than other dominance methods, which leads to a larger selection pressure provided by CN α -dominance.

- Strengthened dominance relation (SDR)

The strengthened dominance relation (SDR) [36] balances the convergence and diversity of the non-dominated solution set by adopting a tailored niching technique. To be Specific, a candidate solution \mathbf{x} is said to dominate another candidate

solution \mathbf{y} based on the SDR (denoted as $\mathbf{x} \prec^{SDR} \mathbf{y}$) if and only if

$$\begin{cases} Con(\mathbf{x}) < Con(\mathbf{y}), & \theta_{\mathbf{xy}} \leq \bar{\theta} \\ Con(\mathbf{x}) \cdot \frac{\theta_{\mathbf{xy}}}{\bar{\theta}} < Con(\mathbf{y}), & \theta_{\mathbf{xy}} > \bar{\theta} \end{cases} \quad (16)$$

where $Con(\mathbf{x}) = \sum_{i=1}^M f_i(\mathbf{x})$ is a metric for measuring the convergence degree of \mathbf{x} , and the parameter analysis of setting $\bar{\theta}$ is referred to the original paper.

It is worth pointing out that the SDR criterion has shown its superiority over the original GPO in [36], however, the AGPO version [45] was not considered in their comparison study.

III. SUPPLEMENTARY RESULTS

A. List of Tables

- Table S-II:** Main properties of 24 test problems.
- Table S-III:** HV results of NSGA-III, MOEA/DD, θ -DEA, 1by1EA, NSGA-II/SDR, and NSGA-III* on DTLZ1–DTLZ7.
- Table S-IV:** Average IGD results of MultiGPO and three variants on 10-objective MaF1–MaF15.
- Table S-V:** Average HV results of MultiGPO and three variants on 10-objective MaF1–MaF15.
- Table S-VI:** IGD results of NSGA-III, MOEA/DD, θ -DEA, 1by1EA, NSGA-II/SDR, and two MultiGPO on WFG1–WFG9.
- Table S-VII:** HV results of NSGA-III, MOEA/DD, θ -DEA, 1by1EA, NSGA-II/SDR, and two MultiGPO on WFG1–WFG9.
- Table S-VIII:** PD results of NSGA-III, MOEA/DD, θ -DEA, 1by1EA, NSGA-II/SDR, and two MultiGPO on WFG1–WFG9.
- Table S-IX:** IGD results of NSGA-III, MOEA/DD, θ -DEA, 1by1EA, NSGA-II/SDR, and two MultiGPO on MaF1–MaF15 with $G_{\max}=500$.
- Table S-X:** HV results of NSGA-III, MOEA/DD, θ -DEA, 1by1EA, NSGA-II/SDR, and two MultiGPO on MaF1–MaF15 with $G_{\max}=500$.
- Table S-XI:** IGD results of all methods on MaF1–MaF15 with $G_{\max}=200$.
- Table S-XII:** HV results of all methods on MaF1–MaF15 with $G_{\max}=200$.

B. List of Figures

- Fig. S-3:** The result of the median IGD among 30 runs obtained by five dominance relation (CDAS-, S-CDAS-, CN α -GPO- and SDR-dominance) based algorithms and our proposed MultiGPO on 3-objective DTLZ2, DTLZ5, and DTLZ7.
- Fig. S-4:** Parallel coordinates of the non-dominated solution set with the median IGD among 30 runs obtained by five dominance relation based algorithms on 10-objective DTLZ2.
- Fig. S-5:** Parallel coordinates of the non-dominated solution set with the median IGD among 30 runs obtained by five dominance relation based algorithms on 10-objective DTLZ7.
- Fig. S-6:** The result of GPO and MultiGPO using different expanding angles (i.e., $\varphi=10, 20, 30$) on 3-objective DTLZ2.
- Fig. S-7:** The result of GPO and MultiGPO using different expanding angles (i.e., $\varphi=10, 20, 30$) on 3-objective DTLZ5.
- Fig. S-8:** The result of GPO and MultiGPO using different expanding angles (i.e., $\varphi=10, 20, 30$) on 3-objective DTLZ7.
- Fig. S-9:** Results of MultiGPO, Variant1 and Variant2 on three-objective MaF3.
- Fig. S-10:** Parallel coordinates of the objective values for each algorithm on ten-objective WFG.
- Fig. S-11:** Parallel coordinates of the objective values for each algorithm on ten-objective MaF (MaF1–9).
- Fig. S-12:** Parallel coordinates of the objective values for each algorithm on ten-objective MaF (MaF10–15).
- Fig. S-13:** Plot results for each algorithm on three-objective MaF (MaF1–8).
- Fig. S-14:** Plot results for each algorithm on three-objective MaF (MaF9–13).

REFERENCES

- [1] M. Asafuddoula, H. K. Singh, and T. Ray, “An enhanced decomposition-based evolutionary algorithm with adaptive reference vectors,” *IEEE Trans. Cybern.*, vol. 48, no. 8, pp. 2321–2334, 2018.
- [2] M. Asafuddoula, T. Ray, and R. Sarker, “A decomposition-based evolutionary algorithm for many objective optimization,” *IEEE Trans. Evol. Comput.*, vol. 19, no. 3, pp. 445–460, 2015.
- [3] Y. Sun, G. G. Yen, and Z. Yi, “Improved regularity model-based EDA for many-objective optimization,” *IEEE Trans. Evol. Comput.*, vol. 22, no. 5, pp. 662–678, 2018.
- [4] X. Cai, Z. Yang, Z. Fan, and Q. Zhang, “A decomposition-based many-objective evolutionary algorithm with two types of adjustments for direction vectors,” *IEEE Trans. Cybern.*, vol. 48, no. 8, pp. 2335–2348, 2018.
- [5] R. Wang, Z. Zhou, H. Ishibuchi, T. Liao, and T. Zhang, “Localized weighted sum method for many-objective optimization,” *IEEE Trans. Evol. Comput.*, vol. 22, no. 1, pp. 3–18, 2018.
- [6] F. Gu and Y. M. Cheung, “Self-organizing map-based weight design for decomposition-based many-objective evolutionary algorithm,” *IEEE Trans. Evol. Comput.*, vol. 22, no. 2, pp. 211–225, 2018.
- [7] H.-L. Liu, L. Chen, Q. Zhang, and K. Deb, “Adaptively allocating search effort in challenging many-objective optimization problems,” *IEEE Trans. Evol. Comput.*, vol. 22, no. 3, pp. 433–448, 2018.
- [8] M. Wu, K. Li, S. Kwong, and Q. Zhang, “Evolutionary many-objective optimization based on adversarial decomposition,” *IEEE Trans. Cybern.*, vol. 50, no. 2, pp. 753–764, 2020.
- [9] Y. Sun, B. Xue, M. Zhang, and G. G. Yen, “A new two-stage evolutionary algorithm for many-objective optimization,” *IEEE Trans. Evol. Comput.*, vol. 23, no. 5, pp. 748–761, 2019.
- [10] Y. Zhou, Y. Xiang, Z. Chen, J. He, and J. Wang, “A scalar projection and angle-based evolutionary algorithm for many-objective optimization problems,” *IEEE Trans. Cybern.*, vol. 49, no. 6, pp. 2073–2084, 2019.
- [11] X.-F. Liu, Z.-H. Zhan, Y. Gao, J. Zhang, S. Kwong, and J. Zhang, “Coevolutionary particle swarm optimization with bottleneck objective learning strategy for many-objective optimization,” *IEEE Trans. Evol. Comput.*, vol. 23, no. 4, pp. 587–602, 2019.
- [12] H. Seada, M. Abouhawwash, and K. Deb, “Multiphase balance of diversity and convergence in multiobjective optimization,” *IEEE Trans. Evol. Comput.*, vol. 23, no. 3, pp. 503–513, 2019.
- [13] C. Liu, Q. Zhao, B. Yan, S. Elsayed, T. Ray, and R. Sarker, “Adaptive sorting-based evolutionary algorithm for many-objective optimization,” *IEEE Trans. Evol. Comput.*, vol. 23, no. 2, pp. 247–257, 2019.
- [14] X. He, Y. Zhou, Z. Chen, and Q. Zhang, “Evolutionary many-objective optimization based on dynamical decomposition,” *IEEE Trans. Evol. Comput.*, vol. 23, no. 3, pp. 361–375, 2019.
- [15] H. Ge, M. Zhao, L. Sun, Z. Wang, G. Tan, Q. Zhang, and C. P. Chen, “A many-objective evolutionary algorithm with two interacting processes: Cascade clustering and reference point incremental learning,” *IEEE Trans. Evol. Comput.*, vol. 23, no. 4, pp. 572–586, 2019.
- [16] M. Elarbi, S. Bechikh, C. A. C. Coello, M. Makhlof, and L. B. Said, “Approximating complex pareto fronts with pre-defined normal-boundary intersection directions,” *IEEE Trans. Evol. Comput.*, to be published. doi: [10.1109/TEVC.2019.2958921](https://doi.org/10.1109/TEVC.2019.2958921).
- [17] L. Chen, H.-L. Liu, K. C. Tan, Y.-M. Cheung, and Y. Wang, “Evolutionary many-objective algorithm using decomposition-based dominance relationship,” *IEEE Trans. Cybern.*, vol. 49, no. 12, pp. 4129–4139, 2019.
- [18] H.-L. Liu, F. Gu, and Q. Zhang, “Decomposition of a multiobjective optimization problem into a number of simple multiobjective subproblems,” *IEEE Trans. Evol. Comput.*, vol. 18, no. 3, pp. 450–455, 2014.
- [19] H. Chen, Y. Tian, W. Pedrycz, G. Wu, R. Wang, and L. Wang, “Hyperplane assisted evolutionary algorithm for many-objective optimization problems,” *IEEE Trans. Cybern.*, vol. 50, no. 7, pp. 3367–3380, 2020.
- [20] Y. H. Zhang, Y. J. Gong, T. L. Gu, H. Q. Yuan, W. Zhang, S. Kwong, and J. Zhang, “DECAL: Decomposition-based coevolutionary algorithm for many-objective optimization,” *IEEE Trans. Cybern.*, vol. 49, no. 1, pp. 27–41, 2019.
- [21] J. Yi, J. Bai, H. He, J. Peng, and D. Tang, “ar-MOEA: A novel preference-based dominance relation for evolutionary multiobjective optimization,” *IEEE Trans. Evol. Comput.*, vol. 23, no. 5, pp. 788–802, 2020.
- [22] Y. Liu, D. Gong, J. Sun, and Y. Jin, “A many-objective evolutionary algorithm using a one-by-one selection strategy,” *IEEE Trans. Cybern.*, vol. 47, no. 9, pp. 2689–2702, 2017.

TABLE S-II
MAIN PROPERTIES OF 24 TEST PROBLEMS

Problem	M	n	Property
WFG1	5,8,10,15,20	$k+l$, $k=M-1$, $l=10$	Mixed, Biased, Scaled
WFG2			Convex, Disconnected, Multi-modal, Non-separable, Scaled
WFG3			Linear, Degenerate, Non-separable, Scaled
WFG4			Concave, Multi-modal, Scaled
WFG5			Concave, Deceptive, Scaled
WFG6			Concave, Non-separable, Scaled
WFG7			Concave, Biased, Scaled
WFG8			Concave, Biased, Non-separable, Scaled
WFG9			Concave, Biased, Multi-modal, Deceptive, Non-separable, Scaled
MaF1	5,8,10,15,20	$M+9$	Linear, No single optimal solution in any subset of objectives
MaF2			Concave, No single optimal solution in any subset of objectives
MaF3			Convex, Multi-modal
MaF4		$M+19$	Concave, Multi-modal, Badly-scaled, No single optimal solution in any subset of objectives
MaF5			Convex, Biased, Badly-scaled
MaF6			Concave, Degenerate
MaF7		2	Mixed, Disconnected, Multi-modal
MaF8			Linear, Degenerate
MaF9			Linear, Degenerate
MaF10		$M+9$	Mixed, Biased
MaF11			Convex, Disconnected, Non-separable
MaF12			Concave, Non-separable, Biased Deceptive
MaF13		5	Concave, Unimodal, Non-separable, Degenerate, Complex Pareto set
MaF14			Linear, Partially separable, Large scale
MaF15		$20 \times M$	Convex, Partially separable, Large scale

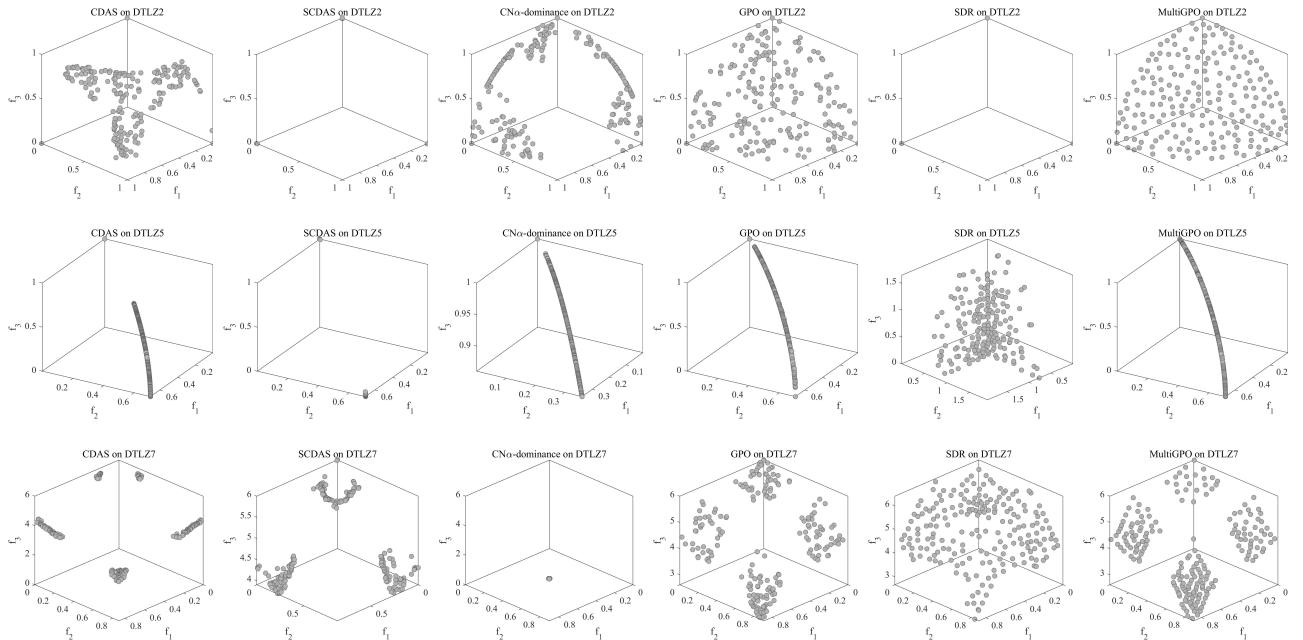


Fig. S-3. The result of the median IGD among 30 runs obtained by five dominance relation (CDAS-, S-CDAS-, CN α - GPO- and SDR-dominance) based algorithms and our proposed MultiGPO on 3-objective DTLZ2, DTLZ5, and DTLZ7.

- [23] Y. Tian, R. Cheng, X. Zhang, F. Cheng, and Y. Jin, "An indicator-based multiobjective evolutionary algorithm with reference point adaptation for better versatility," *IEEE Trans. Evol. Comput.*, vol. 22, no. 4, pp. 609–622, 2018.
- [24] Q. Lin, S. Liu, Q. Zhu, C. Tang, R. Song, J. Chen, C. A. C. Coello, K. C. Wong, and J. Zhang, "Particle swarm optimization with a balanceable fitness estimation for many-objective optimization problems," *IEEE Trans. Evol. Comput.*, vol. 22, no. 1, pp. 32–46, 2018.
- [25] Y. Sun, G. G. Yen, and Z. Yi, "IGD indicator-based evolutionary algorithm for many-objective optimization problems," *IEEE Trans. Evol. Comput.*, vol. 23, no. 2, pp. 173–187, 2019.
- [26] T. Pamulapati, R. Mallipeddi, and P. N. Suganthan, " I_{SDE}^+ —an indicator for multi and many-objective optimization," *IEEE Trans. Evol. Comput.*, vol. 23, no. 2, pp. 346–352, 2019.
- [27] M. Li, S. Yang, and X. Liu, "Shift-based density estimation for pareto-based algorithms in many-objective optimization," *IEEE Trans. Evol. Comput.*, vol. 18, no. 3, pp. 348–365, 2014.
- [28] Y. Tian, X. Zhang, R. Cheng, C. He, and Y. Jin, "Guiding evolutionary multiobjective optimization with generic front modeling," *IEEE Trans. Cybern.*, vol. 50, no. 3, pp. 1106–1119, 2020.
- [29] Z. Liang, K. Hu, X. Ma, and Z. Zhu, "A many-objective evolutionary algorithm based on a two-round selection strategy," *IEEE Trans. Cybern.*, to be published. doi: [10.1109/TCYB.2019.2918087](https://doi.org/10.1109/TCYB.2019.2918087).
- [30] K. Shang and H. Ishibuchi, "A new hypervolume-based evolutionary algorithm for many-objective optimization," *IEEE Trans. Evol. Comput.*, to be published. doi: [10.1109/TEVC.2020.2964705](https://doi.org/10.1109/TEVC.2020.2964705).
- [31] Z. Liang, T. Luo, K. Hu, X. Ma, and Z. Zhu, "An indicator-based many-objective evolutionary algorithm with boundary protection," *IEEE Trans. Cybern.*, to be published. doi: [10.1109/TCYB.2019.2960302](https://doi.org/10.1109/TCYB.2019.2960302).
- [32] H. Xu, W. Zeng, X. Zeng, and G. G. Yen, "A polar-metric-based evolutionary algorithm," *IEEE Trans. Cybern.*, to be published. doi: [10.1109/TCYB.2020.2965230](https://doi.org/10.1109/TCYB.2020.2965230).
- [33] Y. Xiang, Z. Yuren, M. Li, and Z. Chen, "A vector angle based evolutionary algorithm for unconstrained many-objective optimization," *IEEE Trans. Evol. Comput.*, vol. 21, no. 1, pp. 131–152, 2017.
- [34] Y. Xiang, Y. Zhou, Z. Chen, and J. Zhang, "A many-objective particle swarm optimizer with leaders selected from historical solutions by using scalar projections," *IEEE Trans. Cybern.*, vol. 50, no. 5, pp. 2209–2222,

TABLE S-III
HV RESULTS OF NSGA-III, MOEA/DD, θ -DEA, 1BY1EA, NSGA-II/SDR, AND NSGA-III* ON DTLZ1–DTLZ7. THE BEST RESULT FOR EACH TEST INSTANCE IS SHOWN WITH DARK BACKGROUND.

Problem	M	NSGA-III	MOEA/DD	θ -DEA	1by1EA	NSGA-II/SDR	NSGA-III*
DTLZ1	5	9.7964e-1 (1.67e-4) \approx	9.7978e-1 (1.20e-4) \approx	9.7973e-1 (1.77e-4) \approx	9.3807e-1 (6.76e-3) —	9.4135e-1 (1.06e-2) —	9.7974e-1 (2.21e-4)
	10	9.7544e-1 (4.69e-2) \approx	9.9951e-1 (6.14e-5) \approx	9.9938e-1 (5.13e-4) —	9.9209e-1 (1.52e-3) —	9.4803e-1 (1.50e-2) —	9.9957e-1 (7.82e-4)
	15	9.9685e-1 (4.61e-3) \approx	9.651e-1 (9.00e-3) —	9.8532e-1 (2.65e-2) —	9.9664e-1 (3.95e-4) —	8.7224e-1 (5.62e-2) —	9.9985e-1 (3.40e-5)
DTLZ2	5	8.1241e-1 (3.32e-4) \approx	8.1248e-1 (4.39e-4) \approx	8.1255e-1 (3.71e-4) \approx	8.0071e-1 (2.19e-3) —	7.9402e-1 (3.09e-3) —	8.1230e-1 (3.73e-4)
	10	9.5692e-1 (1.89e-2) \approx	9.6960e-1 (1.19e-4) +	9.6960e-1 (1.17e-4) —	9.5551e-1 (2.09e-3) —	9.6437e-1 (1.50e-3) +	9.6266e-1 (1.93e-2)
	15	9.8017e-1 (6.57e-3) \approx	9.2859e-1 (1.18e-2) —	9.9073e-1 (1.48e-4) +	9.7831e-1 (1.81e-3) \approx	9.8818e-1 (2.40e-3) +	9.7915e-1 (1.12e-2)
DTLZ3	5	7.9429e-1 (8.79e-3) \approx	8.0159e-1 (4.85e-3) \approx	8.0428e-1 (4.90e-3) +	7.9753e-1 (1.91e-3) \approx	7.9407e-1 (3.77e-3) —	7.9915e-1 (6.92e-3)
	10	4.9439e-1 (4.31e-1) —	9.6365e-1 (3.16e-3) \approx	9.0746e-1 (1.08e-1) \approx	9.5214e-1 (3.30e-3) \approx	9.6223e-1 (1.92e-3) +	9.4403e-1 (2.72e-2)
	15	2.0456e-1 (3.49e-1) —	8.9487e-1 (2.27e-2) \approx	9.3338e-1 (1.07e-1) +	9.7805e-1 (2.19e-3) +	9.8526e-1 (3.53e-3) +	7.5982e-1 (3.69e-1)
DTLZ4	5	8.1209e-1 (5.60e-4) \approx	8.1253e-1 (3.24e-4) +	8.1261e-1 (3.81e-4) +	8.0768e-1 (1.71e-3) —	3.7487e-1 (5.44e-2) —	8.1223e-1 (4.18e-4)
	10	9.6936e-1 (2.38e-4) —	9.6984e-1 (1.59e-4) \approx	9.6994e-1 (1.79e-4) \approx	9.6322e-1 (2.86e-3) —	5.4932e-1 (7.99e-2) —	9.7003e-1 (3.35e-4)
	15	9.8503e-1 (5.36e-3) —	9.9091e-1 (1.56e-4) —	9.9130e-1 (7.10e-5) —	9.8909e-1 (5.90e-4) —	7.7334e-1 (3.35e-2) —	9.9157e-1 (1.19e-4)
DTLZ5	5	1.1287e-1 (5.37e-3) —	1.1551e-1 (2.91e-4) —	1.0124e-1 (7.06e-3) —	1.2462e-1 (3.30e-3) +	1.0863e-1 (4.09e-3) —	1.1789e-1 (1.71e-3)
	10	8.8277e-2 (2.95e-3) —	9.3851e-2 (4.77e-4) \approx	9.3728e-2 (1.33e-3) \approx	9.0302e-2 (4.04e-3) —	8.9884e-2 (8.59e-4) —	9.4348e-2 (1.46e-3)
	15	8.3430e-2 (5.51e-3) —	9.1818e-2 (5.23e-4) +	9.0776e-2 (7.64e-4) \approx	8.6867e-2 (4.83e-3) —	9.0084e-2 (6.68e-4) —	9.1024e-2 (7.63e-4)
DTLZ6	5	1.0345e-1 (9.29e-3) —	1.1503e-1 (4.56e-4) +	9.5385e-2 (4.95e-3) —	1.1671e-1 (3.05e-3) +	1.1241e-1 (3.49e-3) \approx	1.1014e-1 (7.31e-3)
	10	6.3626e-2 (4.39e-2) —	9.4313e-2 (2.47e-4) —	9.0892e-2 (1.04e-4) —	3.1697e-2 (2.95e-2) —	8.5937e-2 (1.09e-2) —	9.3034e-2 (1.99e-3)
	15	1.8129e-2 (3.82e-2) —	9.0906e-2 (5.40e-4) \approx	9.0791e-2 (3.42e-4) —	1.3843e-2 (1.76e-2) —	9.1023e-2 (3.71e-4) \approx	9.1289e-2 (4.97e-4)
DTLZ7	5	2.5645e-1 (4.29e-3) —	9.7561e-2 (2.12e-2) —	2.1384e-1 (8.57e-3) —	1.9781e-1 (1.36e-2) —	2.5758e-1 (3.34e-3) —	2.6005e-1 (3.70e-3)
	10	1.7011e-1 (7.34e-3) —	9.2944e-5 (5.87e-5) —	1.9049e-1 (5.36e-3) \approx	6.2061e-2 (8.63e-3) —	1.6682e-1 (5.38e-3) —	1.9069e-1 (2.01e-3)
	15	8.1898e-2 (2.87e-2) +	3.6246e-7 (2.50e-8) —	8.7977e-2 (1.93e-2) +	1.1874e-4 (1.16e-4) —	9.5337e-9 (3.01e-8) —	6.8549e-2 (2.92e-2)

+, – and \approx indicate that the result is significantly better, significantly worse and statistically similar to that obtained by NSGA-III*, respectively.

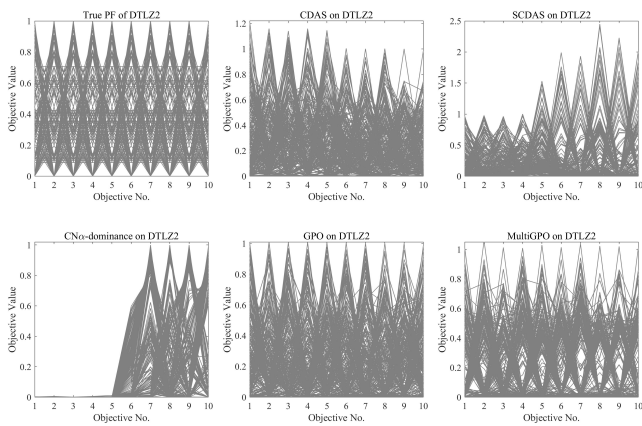


Fig. S-4. Parallel coordinates of the non-dominated solution set with the median IGD among 30 runs obtained by five dominance relation based algorithms on 10-objective DTLZ2.

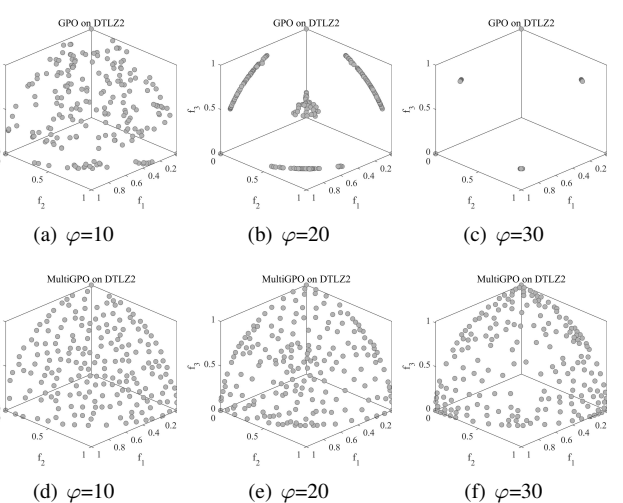


Fig. S-6. The result of GPO and MultiGPO using different expanding angles (i.e., $\varphi=10, 20, 30$) on 3-objective DTLZ2.

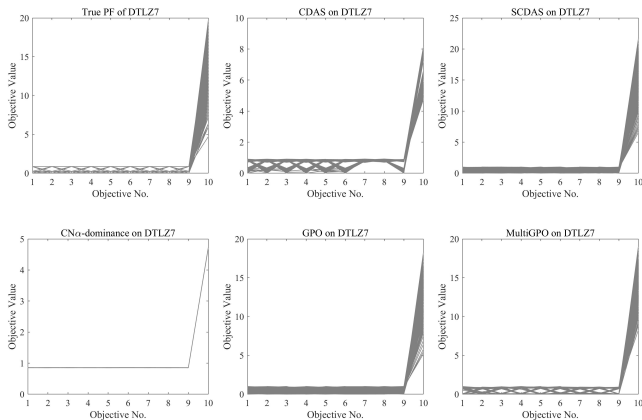


Fig. S-5. Parallel coordinates of the non-dominated solution set with the median IGD among 30 runs obtained by five dominance relation based algorithms on 10-objective DTLZ7.

- [2020]
- [35] Q. Lin, S. Liu, K.-C. Wong, M. Gong, C. A. Coello Coello, J. Chen, and J. Zhang, "A clustering-based evolutionary algorithm for many-objective optimization problems," *IEEE Trans. Evol. Comput.*, vol. 23, no. 3, pp. 391–405, 2019.
- [36] Y. Tian, R. Cheng, X. Zhang, Y. Su, and Y. Jin, "A strengthened dominance relation considering convergence and diversity for evolutionary many-objective optimization," *IEEE Trans. Evol. Comput.*, vol. 23, no. 2, pp. 331–345, 2019.
- [37] H. Xu, W. Zeng, X. Zeng, and G. G. Yen, "An evolutionary algorithm based on minkowski distance for many-objective optimization," *IEEE Trans. Cybern.*, vol. 49, no. 11, pp. 3968–3979, 2019.
- [38] L. Li, L. Chang, T. Gu, W. Sheng, and W. Wang, "On the norm of dominant difference for many-objective particle swarm optimization," *IEEE Trans. Cybern.*, to be published. doi: [10.1109/TCYB.2019.2922287](https://doi.org/10.1109/TCYB.2019.2922287).
- [39] Y. Xiang, Y. Zhou, X. Yang, and H. Huang, "A many-objective evolutionary algorithm with pareto-adaptive reference points," *IEEE Trans. Evol. Comput.*, vol. 24, no. 1, pp. 99–113, 2020.
- [40] K. Zhang, Z. Xu, S. Xie, and G. G. Yen, "Evolution strategy-based many-objective evolutionary algorithm through vector equilibrium," *IEEE Trans. Cybern.*, to be published. doi:

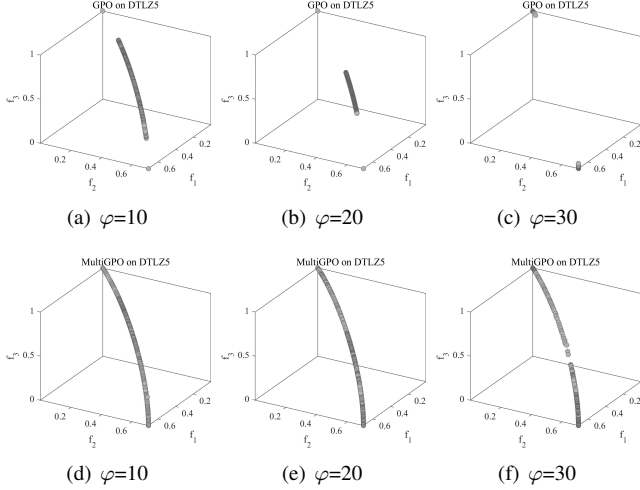


Fig. S-7. The result of GPO and MultiGPO using different expanding angles (i.e., $\varphi=10, 20, 30$) on 3-objective DTLZ5.

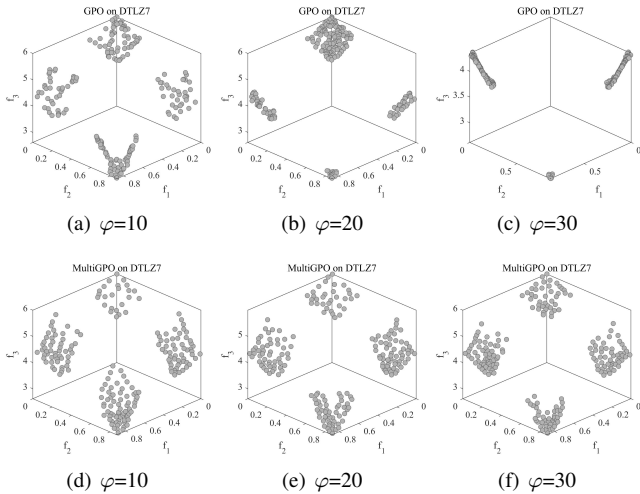


Fig. S-8. The result of GPO and MultiGPO using different expanding angles (i.e., $\varphi=10, 20, 30$) on 3-objective DTLZ7.

10.1109/TCYB.2019.2960039.

- [41] L. S. Batista, F. Campelo, F. G. Guimarães, and J. A. Ramírez, “Pareto cone ε -dominance: improving convergence and diversity in multiobjective evolutionary algorithms,” in *Proc. Int. Conf. Evolutionary Multi-Criterion Optimization*. Springer, 2011, pp. 76–90.
- [42] H. Sato, H. E. Aguirre, and K. Tanaka, “Controlling dominance area of solutions and its impact on the performance of MOEAs,” in *Proc. Int. Conf. Evolutionary Multi-criterion Optimization*. ACM, 2007, pp. 5–20.
- [43] H. Sato, H. Aguirre, and K. Tanaka, “Self-controlling dominance area of solutions in evolutionary many-objective optimization,” *Simulated Evolution and Learning*, pp. 455–465, 2010.
- [44] J. Liu, Y. Wang, X. Wang, S. Guo, and X. Sui, “A new dominance method based on expanding dominated area for many-objective optimization,” *Intern. J. Pattern Recognit. Artif. Intell.*, vol. 33, no. 03, p. 1959008, 2019.
- [45] C. Zhu, L. Xu, and E. D. Goodman, “Generalization of pareto-optimality for many-objective evolutionary optimization,” *IEEE Trans. Evol. Comput.*, vol. 20, no. 2, pp. 299–315, 2016.
- [46] K. Deb, M. Mohan, and S. Mishra, “Evaluating the ε -domination based multi-objective evolutionary algorithm for a quick computation of pareto-optimal solutions,” *Evol. Comput.*, vol. 13, no. 4, pp. 501–525, 2005.
- [47] S. K. K. Ikeda, H. Kita, “Failure of pareto-based moeas: does non-dominated really mean near to optimal?” in *Proc. of the 2001 Congress on Evolutionary Computation*, vol. 2, 2001, pp. 957–962.

TABLE S-IV
AVERAGE IGD RESULTS OF MULTIGPO AND THREE VARIANTS ON 10-OBJECTIVE MAF1–MAF15. THE BEST RESULT FOR EACH TEST INSTANCE IS SHOWN IN BOLD FONT.

Problem	MultiGPO	Variant1	Variant2	Variant3
MaF1	2.305e-1	2.320e-1 ≈	2.326e-1 ≈	2.515e-1 –
MaF2	1.814e-1	2.016e-1 –	1.846e-1 ≈	1.778e-1 ≈
MaF3	1.895e+3	2.971e+2 +	7.050e+1 +	6.555e+2 +
MaF4	6.072e+1	5.972e+1 +	5.331e+1 +	5.475e+1 +
MaF5	1.956e+2	1.999e+2 ≈	1.941e+2 ≈	1.657e+2 +
MaF6	8.401e-2	1.689e-1 –	1.411e-1 –	1.490e-1 –
MaF7	8.953e-1	9.120e-1 –	8.674e-1 +	8.744e-1 +
MaF8	1.028e-1	1.037e-1 ≈	1.015e-1 ≈	9.953e-2 ≈
MaF9	9.746e-2	9.753e-2 ≈	9.736e-2 ≈	9.835e-2 ≈
MaF10	1.104e+0	1.024e+0 +	1.177e+0 –	9.879e-1 +
MaF11	1.474e+0	1.239e+0 +	1.267e+0 +	1.486e+0 ≈
MaF12	3.983e+0	3.999e+0 ≈	3.983e+0 ≈	4.037e+0 ≈
MaF13	1.443e-1	1.201e-1 +	1.222e-1 –	1.326e-1 +
MaF14	7.786e-1	7.629e-1 ≈	7.960e-1 ≈	8.335e-1 ≈
MaF15	1.211e+0	1.095e+0 ≈	1.135e+0 ≈	1.257e+0 ≈
+ / - / ≈		5/3/7	5/2/8	6/2/7

+, – and ≈ indicate that the result is significantly better, significantly worse and statistically similar to that obtained by MultiGPO, respectively.

TABLE S-V
AVERAGE HV RESULTS OF MULTIGPO AND THREE VARIANTS ON 10-OBJECTIVE MAF1–MAF15. THE BEST RESULT FOR EACH TEST INSTANCE IS SHOWN IN BOLD FONT.

Problem	MultiGPO2	Variant1	Variant2	Variant3
MaF1	3.471e-7	5.984e-7 ≈	4.665e-7 ≈	9.282e-8 –
MaF2	2.263e-1	2.444e-1 +	2.240e-1 ≈	2.356e-1 ≈
MaF3	2.769e-1	2.080e-1 –	4.864e-1 +	1.185e-1 –
MaF4	8.466e-5	8.053e-5 ≈	6.462e-5 –	4.340e-5 –
MaF5	9.122e-1	8.994e-1 –	9.103e-1 ≈	9.138e-1 ≈
MaF6	6.121e-2	7.519e-2 +	5.873e-2 –	6.213e-2 +
MaF7	9.403e-2	1.131e-1 +	9.374e-2 ≈	8.834e-2 –
MaF8	1.120e-2	1.120e-2 ≈	1.116e-2 ≈	1.104e-2 ≈
MaF9	1.882e-2	1.871e-2 ≈	1.866e-2 ≈	1.852e-2 ≈
MaF10	9.979e-1	9.989e-1 ≈	9.996e-1 ≈	9.986e-1 ≈
MaF11	9.881e-1	9.939e-1 ≈	9.944e-1 ≈	9.930e-1 ≈
MaF12	8.852e-1	9.137e-1 +	8.918e-1 ≈	8.850e-1 ≈
MaF13	1.320e-1	1.309e-1 –	1.294e-1 –	1.310e-1 ≈
MaF14	6.026e-1	5.367e-1 –	5.517e-1 –	5.293e-1 –
MaF15	4.224e-9	6.759e-9 +	8.007e-9 +	1.18e-10 –
+ / - / ≈		5/4/6	2/4/9	1/6/8

+, – and ≈ indicate that the result is significantly better, significantly worse and statistically similar to that obtained by MultiGPO2, respectively.

- [48] C. Dai, Y. Wang, and L. Hu, “An improved α -dominance strategy for many-objective optimization problems,” *Soft Comput.*, vol. 20, no. 3, pp. 1105–1111, 2016.

TABLE S-VI

IGD RESULTS OF NSGA-III, MOEA/DD, θ -DEA, 1BY1EA, NSGA-II/SDR, AND TWO MULTIGPO ON WFG1–WFG9. THE BEST AND THE RESULT THAT IS STATISTICALLY SIMILAR TO THE BEST FOR EACH TEST INSTANCE ARE SHOWN WITH DARK AND LIGHT GRAY BACKGROUND, RESPECTIVELY.

Problem	M	NSGA-III	MOEA/DD	θ -DEA	1by1EA	NSGA-II/SDR	MultiGPO	MultiGPO2
WFG1	5	1.1858e+0 (8.50e-2) ≈	1.3815e+0 (8.40e-2) —	8.8850e-1 (5.46e-2) +	1.0758e+0 (9.90e-2) ≈	8.3275e-1 (8.42e-2) +	1.1860e+0 (1.66e-1)	8.6543e-1 (9.51e-2) +
	8	1.9647e+0 (1.32e-1) —	2.3254e+0 (1.69e-1) —	1.3964e+0 (1.09e-1) +	1.8322e+0 (1.49e-1) —	1.4769e+0 (1.11e-1) —	1.6553e+0 (1.85e-1)	1.5674e+0 (9.35e-2) ≈
	10	2.1515e+0 (1.53e-1) —	2.0129e+0 (1.33e-1) —	1.4303e+0 (1.35e-1) +	2.0987e+0 (1.24e-1) —	1.5941e+0 (7.89e-2) +	1.7137e+0 (1.62e-1)	1.7104e+0 (5.20e-2) ≈
	15	2.8272e+0 (1.32e-1) —	3.1901e+0 (2.95e-1) —	2.9379e+0 (1.94e-1) —	2.2373e+0 (6.36e-2) ≈	2.2579e+0 (2.16e-1) —	2.1493e+0 (2.13e-1) ≈	
	20	4.7319e+0 (1.69e-1) —	4.6996e+0 (9.67e-2) —	3.9946e+0 (1.65e-1) ≈	4.7913e+0 (1.27e-1) —	5.0313e+0 (5.72e-2) —	3.9820e+0 (3.26e-1)	3.8836e+0 (3.09e-1) ≈
WFG2	5	8.8719e-1 (4.16e-3) ≈	4.7628e-1 (1.32e-2) ≈	3.8747e-1 (3.68e-3) ≈	6.3224e-1 (6.23e-2) —	4.9537e-1 (5.67e-2) —	4.3332e-1 (1.33e-1) —	6.3339e-1 (1.13e-1) —
	8	9.4422e-1 (1.70e-1) —	1.1334e+0 (3.42e-2) +	9.2618e-1 (1.13e-1) —	1.6352e+0 (9.59e-2) —	1.3863e+0 (1.40e-1) —	1.2315e+0 (8.88e-2)	1.7323e+0 (1.28e-1)
	10	1.3163e+0 (2.38e-1) ≈	1.3154e+0 (3.38e-2) +	1.1602e+0 (1.25e-1) +	1.7501e+0 (9.29e-2) —	1.6024e+0 (1.25e-1) —	1.4220e+0 (6.94e-2)	1.9270e+0 (4.68e-2)
	15	1.5520e+0 (6.88e-2) +	1.9313e+0 (5.41e-2) +	3.7622e+0 (1.42e-2) +	2.2463e+0 (5.34e-2) +	2.3754e+0 (9.95e-2) +	2.1438e+0 (1.09e-1)	2.4313e+0 (1.16e-1)
	20	3.9117e+0 (1.84e-1) —	5.4387e+0 (7.63e-2) —	4.8707e+0 (9.11e-1) —	4.6407e+0 (1.92e-1) —	5.1564e+0 (8.27e-2) —	4.3854e+0 (2.08e-1)	4.9847e+0 (2.61e-1)
WFG3	5	4.6479e-1 (4.05e-2) +	5.9652e-1 (4.40e-2) +	4.7830e-1 (3.20e-2) +	1.3427e+0 (1.26e-1) —	3.8019e-1 (5.05e-2) +	8.7851e-1 (1.11e-1) —	8.5208e-1 (1.47e-1) ≈
	8	1.5909e+0 (2.51e-1) +	2.2091e+0 (1.61e-1) ≈	8.7188e-1 (1.52e-1) +	3.6317e+0 (2.93e-1) —	9.3824e-1 (1.78e-1) +	2.2347e+0 (5.75e-1) —	2.0262e+0 (4.57e-1) ≈
	10	1.2223e+0 (3.54e-1) —	2.7216e+0 (1.14e-1) —	1.0917e+0 (1.21e-1) —	5.5450e+0 (5.70e-1) —	1.7902e+0 (9.85e-1) —	2.5192e+0 (5.55e-1) —	2.2814e+0 (5.92e-1) —
	15	2.1099e+0 (3.73e-1) +	5.9627e+0 (2.76e-1) +	2.0588e+0 (1.90e-1) +	1.0296e+1 (1.94e+0) +	3.7524e+0 (0.95e-1) +	2.8032e+0 (7.42e-1) —	2.6523e+0 (7.70e-1) ≈
	20	6.1407e+0 (2.29e+0) +	1.9747e+1 (2.60e+0) +	3.4151e+0 (4.90e-1) +	1.4000e+1 (2.21e+0) +	8.8356e+0 (2.58e+0) +	1.6761e+0 (3.30e-1) +	1.7033e+0 (3.58e-1) ≈
WFG4	5	9.6515e-1 (2.63e-3) —	1.0520e+0 (2.91e-3) —	9.6623e-1 (3.53e-3) —	1.4610e+0 (1.29e-1) —	9.9227e-1 (8.42e-3) —	9.5382e-1 (8.39e-3) —	9.8554e-1 (1.35e-2) —
	8	2.7567e+0 (1.05e-2) +	3.3613e+0 (9.13e-2) +	2.7591e+0 (8.68e-3) —	3.9718e+0 (1.47e-1) —	2.8762e+0 (2.46e-2) —	2.7083e+0 (2.62e-2) —	2.7235e+0 (3.17e-2) ≈
	10	4.5265e+0 (2.05e-2) —	6.1034e+0 (1.68e-1) —	4.5221e+0 (1.41e-2) +	5.8503e+0 (1.73e-1) —	4.3519e+0 (1.56e-2) —	4.0438e+0 (3.37e-2) —	4.0790e+0 (4.34e-2) —
	15	8.1436e+0 (1.34e-1) —	9.1569e+0 (3.43e-1) —	8.1272e+0 (6.50e-2) —	1.0761e+1 (2.90e-1) —	8.0536e+0 (1.77e-1) —	7.3919e+0 (9.40e-2) —	7.4621e+0 (7.89e-2) —
	20	1.4378e+1 (1.31e+0) +	1.1428e+1 (4.90e-1) +	1.1363e+1 (8.11e-2) +	1.5285e+1 (6.29e-2) —	1.6895e+1 (2.80e+0) —	1.1876e+1 (3.14e-1) —	1.1078e+1 (1.70e-1) +
WFG5	5	9.4880e-1 (3.52e-3) ≈	1.0318e+0 (5.53e-3) ≈	9.4727e-1 (3.43e-3) +	1.4000e+0 (1.11e-1) —	9.8690e-1 (1.32e-2) —	9.5024e-1 (7.74e-3) —	9.8618e-1 (1.74e-2) —
	8	2.7624e+0 (7.92e-3) ≈	3.2371e+0 (5.31e-2) +	2.7711e+0 (8.39e-3) —	3.9969e+0 (1.48e-1) —	2.9260e+0 (3.64e-2) —	2.7534e+0 (3.00e-2) —	2.7831e+0 (3.61e-2) —
	10	4.4659e+0 (1.80e-2) +	6.2316e+0 (1.14e-1) +	4.4542e+0 (1.62e-2) +	5.9729e+0 (1.78e-1) —	4.4108e+0 (5.55e-2) —	4.0335e+0 (4.00e-2) —	4.1443e+0 (4.13e-2) —
	15	7.9602e+0 (2.47e-1) —	9.3904e+0 (1.98e-1) —	7.6200e+0 (1.01e-1) —	1.1121e+1 (2.17e-1) —	8.0924e+0 (2.72e-1) —	7.2058e+0 (7.17e-2) —	7.1997e+0 (7.16e-2) ≈
	20	1.2613e+1 (5.23e-1) —	1.8609e+1 (3.61e-1) —	1.1168e+1 (2.47e-2) —	1.5592e+1 (2.74e-1) —	1.2404e+1 (1.26e-0) —	1.1477e+1 (1.77e-1) —	1.0865e+1 (1.96e-1) +
WFG6	5	9.6632e-1 (3.53e-3) +	1.0498e+0 (4.48e-3) +	9.6442e-1 (2.59e-3) +	1.7801e+0 (1.21e-1) —	1.0018e+0 (1.13e-2) —	1.0114e+0 (1.71e-2) —	1.0728e+0 (4.72e-2) —
	8	2.7844e+0 (8.10e-3) +	3.3466e+0 (7.29e-2) +	2.7836e+0 (5.92e-3) +	4.6839e+0 (1.00e-1) —	3.0577e+0 (5.75e-2) —	2.8959e+0 (4.59e-2) —	2.9823e+0 (4.65e-2) —
	10	4.5584e+0 (2.20e-2) +	6.0128e+0 (1.72e-1) +	4.5717e+0 (1.38e-2) +	6.8302e+0 (1.82e-1) —	4.5433e+0 (6.48e-2) —	4.2468e+0 (1.08e-1) —	4.3654e+0 (1.04e-1) —
	15	8.0353e+0 (1.70e-1) +	1.0502e+1 (3.70e-1) +	7.9722e+0 (1.43e-1) +	1.2642e+1 (3.87e-1) —	8.2217e+0 (2.50e-1) —	7.4390e+0 (4.46e-1) —	7.9619e+0 (5.80e-1) —
	20	1.3412e+1 (7.73e-1) +	1.5407e+1 (3.10e+0) +	1.1458e+1 (1.86e-1) +	1.7421e+1 (7.76e-1) —	1.6745e+1 (3.29e+0) —	1.1356e+1 (2.26e-1) —	1.0813e+1 (3.74e-1) +
WFG7	5	9.6536e-1 (2.60e-3) —	1.0498e+0 (4.48e-3) —	9.6442e-1 (2.59e-3) +	1.7801e+0 (1.21e-1) —	1.0018e+0 (1.13e-2) —	1.0114e+0 (1.71e-2) —	1.0728e+0 (4.72e-2) —
	8	2.7530e+0 (1.03e-2) —	3.1381e+0 (4.90e-2) +	2.7518e+0 (8.23e-3) —	4.6839e+0 (1.00e-1) —	3.0577e+0 (5.75e-2) —	2.8959e+0 (4.59e-2) —	2.9823e+0 (4.65e-2) —
	10	4.5126e+0 (4.46e-2) —	5.1228e+0 (2.40e-1) —	4.5420e+0 (2.49e-2) —	6.0670e+0 (2.50e-1) —	4.4079e+0 (5.83e-2) —	4.0466e+0 (3.33e-2) —	4.2428e+0 (3.75e-2) —
	15	8.1856e+0 (8.00e-2) —	7.9308e+0 (4.47e-1) —	8.2404e+0 (9.50e-2) —	9.6971e+0 (3.06e-1) —	1.0124e+1 (1.58e-0) —	7.2578e+0 (7.01e-2) —	7.6162e+0 (1.20e-1) —
	20	1.6936e+1 (1.01e+0) +	1.5407e+1 (3.10e+0) +	1.1458e+1 (1.86e-1) +	1.5390e+1 (2.30e-1) —	1.4209e+1 (9.45e-1) —	1.1905e+1 (1.96e-1) —	1.1321e+1 (9.47e-2) +
WFG8	5	1.0051e+0 (7.65e-3) +	1.0718e+0 (7.00e-3) +	9.9730e-1 (1.95e-3) +	1.3842e+0 (1.41e-1) —	9.9804e-1 (1.40e-2) —	9.6155e-1 (8.73e-3) —	1.0316e+0 (9.25e-2) —
	8	3.1427e+0 (3.87e-2) ≈	3.3392e+0 (7.09e-2) ≈	3.1146e+0 (2.98e-2) ≈	4.3355e+0 (1.62e-2) —	2.9403e+0 (3.14e-2) —	2.8167e+0 (2.10e-2) —	
	10	4.5060e+0 (3.01e-1) ≈	5.2796e+0 (3.13e-1) ≈	4.3198e+0 (2.06e-2) ≈	4.5903e+0 (2.78e-1) —	3.0262e+0 (3.40e-2) —	3.1219e+0 (4.43e-2) —	3.0798e+0 (3.78e-2) —
	15	8.4233e+0 (5.10e-1) +	1.0484e+1 (2.93e-1) +	8.3975e+0 (4.80e-1) +	1.1063e+1 (1.03e-0) +	8.9308e+0 (1.44e-0) ≈	8.7948e+0 (1.78e-1) —	8.7223e+0 (3.19e-1) ≈
	20	1.7393e+1 (1.59e+0) +	1.2070e+1 (5.10e+0) +	1.3309e+1 (3.29e-1) +	1.4909e+1 (1.29e+0) ≈	1.4159e+1 (2.06e+0) ≈	1.4429e+1 (2.93e-1) —	1.3167e+1 (2.17e-1) +
WFG9	5	9.3516e-1 (4.95e-3) —	1.0425e+0 (6.25e-3) —	9.2847e-1 (4.91e-3) ≈	1.3641e+0 (1.08e-1) —	9.7281e-1 (8.80e-3) —	9.2598e-1 (5.45e-3) —	9.4438e-1 (1.37e-2) —
	8	2.8091e+0 (3.75e-2) +	3.2399e+0 (5.84e-2) +	2.7806e+0 (1.80e-2) —	3.7200e+0 (1.12e-2) —	2.8800e+0 (2.94e-2) —	2.7667e+0 (1.43e-2) —	2.7368e+0 (2.10e-2) +
	10	4.3202e+0 (7.46e-2) +	5.2658e+0 (2.85e-1) +	4.2850e+0 (3.76e-2) +	5.4574e+0 (1.89e-2) +	4.2823e+0 (4.19e-2) —	3.9938e+0 (2.83e-2) —	4.0456e+0 (4.45e-2) —
	15	8.1163e+0 (1.37e-1) +	8.9071e+0 (2.39e-1) +	7.6000e+0 (1.45e-1) +	7.6576e+0 (3.59e-1) +	7.6357e+0 (1.47e-1) +	7.0566e+0 (1.20e-1) —	7.0621e+0 (1.02e-1) ≈
	20	1.4556e+1 (1.09e+0) +	1.2340e+1 (1.25e+0) +	1.1944e+1 (1.54e-1) +	1.3417e+1 (2.11e-1) +	1.3235e+1 (9.99e-1) +	1.1804e+1 (2.18e-1) —	1.1136e+1 (2.09e-1) +
+ / - / ≈		11/26/8	8/35/2	16/19/10	0/43/2	8/32/7	11/21/13	
vs MultiGOP2		18/24/3	7/38/0	20/19/6	4/40/1	11/25/9	21/11/13	

+, -, and ≈ indicate that the result is significantly better, significantly worse and statistically similar to that obtained by MultiGPO or MultiGOP2, respectively. These symbols are the same to all next Tables.

TABLE S-VII

HV RESULTS OF NSGA-III, MOEA/DD, θ -DEA, 1BY1EA, NSGA-II/SDR, AND TWO MULTIGPO ON WFG1–WFG9. THE BEST AND THE RESULT THAT IS STATISTICALLY SIMILAR TO THE BEST FOR EACH TEST INSTANCE ARE SHOWN WITH DARK AND LIGHT GRAY BACKGROUND, RESPECTIVELY.

Problem	M	NSGA-III	MOEA/DD	θ -DEA	1by1EA	NSGA-II/SDR	MultiGPO	MultiGPO2
WFG1	5	5.4698e-1 (3.20e-2) —	4.7923e-1 (3.52e-2) —	6.4799e-1 (3.08e-2) —	6.1327e-1 (4.57e-2) —	7.1162e-1 (3.95e-2) ≈	5.2719e-1 (6.14e-2) —	7.0032e-1 (5.80e-2) +
	8	9.8262e-1 (2.65e-3) +	9.6008e-1 (6.10e-3) +	9.8136e-1 (3.00e-3) +	9.7320e-1 (3.23e-2) +	9.6947e-1 (6.21e-3) +	9.8090e-1 (2.44e-3) +	9.7752e-1 (3.16e-3) +
	10	1.2289e-1 (1.94e-2) +	7.4466e-1 (2.35e-2) +	1.5615e-1 (2.16e-2) +	3.9412e-2 (1.26e-2) +	1.7073e-1 (2.13e-2) +	2.6743e-2 (1.92e-2) +	2.8653e-2 (2.76e-2) +
	15	7.7658e-1 (4.06e-2) ≈	7.5630e-1 (4.24e-2) —	7.7993e-1 (2.37e-3) +	6.7338e-1 (1.82e-2) —	7.7673e-1 (3.44e-2) ≈	7.3635e-1 (5.85e-3) —	7.7590e-1 (5.65e-3) —
	20	1.4378e+1 (1.31e+0) +	1.1428e+1 (4.90e-1) +	1.1363e+1 (8.11e-2) +	1.5285e+1 (6.29e-2) —	1.6895e+1 (2.80e+0) —	1.1905e+1 (1.96e-1) —	1.1321e+1 (9.47e-2) +
WFG2	5	1.0051e+0 (7.65e-3) +	1.0718e+0 (7.00e-3) +	9.9730e-1 (1.95e-3) +	1.3842e+0 (1.41e-1) —	9.9804e-1 (1.40e-2) —	9.6155e-1 (8.73e-3) —	1.0650e+0 (1.13e-2) +
	8	3.1427e+0 (3.87e-2) ≈	3.3392e+0 (7.09e-2) ≈	3.1146e+0 (2.98e-2) ≈	4.3355e+0 (1.62e-2) —	2.9403e+0 (3.14e-2) —	2.8167e+0 (2.10e-2) —	
	10	4.5060e+0 (3.01e-1) ≈	5.2796e+0 (3.13e-1) ≈	4.3198e+0 (2.06e-2) ≈	4.5903e+			

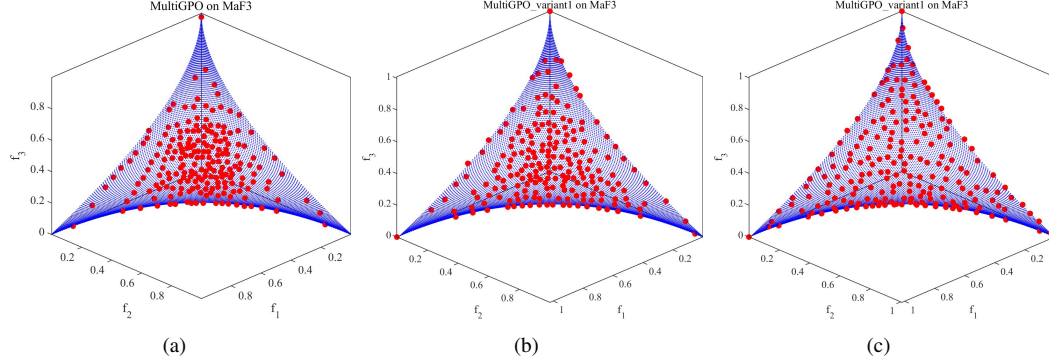


Fig. S-9. Results of MultiGPO, Variant1 and Variant2 on three-objective MaF3.

TABLE S-VIII

PD RESULTS OF NSGA-III, MOEA/DD, θ -DEA, 1by1EA, NSGA-II/SDR, AND TWO MULTIGPO ON WFG1–WFG9. THE BEST AND THE RESULT THAT IS STATISTICALLY SIMILAR TO THE BEST FOR EACH TEST INSTANCE ARE SHOWN WITH DARK AND LIGHT GRAY BACKGROUND, RESPECTIVELY.

Problem	M	NSGA-III	MOEA/DD	θ -DEA	1by1EA	NSGA-II/SDR	MultiGPO	MultiGPO2
WFG1 WFG2 WFG3 WFG4 WFG5 WFG6 WFG7 WFG8 WFG9	5	1.2031e+8 (7.10e+6) ≈	6.9445e+7 (6.47e+6) —	1.0906e+8 (6.09e+6) —	9.2064e+7 (1.11e+7) —	8.8430e+7 (5.81e+6) —	1.1622e+8 (7.41e+6) —	1.0067e+8 (8.23e+6) —
		1.0695e+8 (3.82e+6) —	8.2640e+7 (2.63e+6) —	9.7649e+7 (3.38e+6) —	8.9793e+7 (3.89e+6) —	8.7453e+7 (5.47e+6) —	1.2041e+8 (1.56e+7) —	9.9830e+7 (1.48e+7) —
		2.0544e+8 (8.09e+6) —	1.4434e+8 (6.07e+6) —	1.3474e+8 (1.05e+7) —	2.2215e+8 (5.57e+6) —	2.1456e+8 (7.38e+6) —	2.6121e+8 (7.13e+6) —	2.3855e+8 (5.79e+6) ≈
		2.1135e+8 (5.32e+6) —	1.8571e+8 (4.80e+6) —	2.0733e+8 (4.97e+6) —	2.4698e+8 (1.49e+7) —	3.1250e+8 (1.66e+7) —	3.8962e+8 (9.84e+6) —	3.5297e+8 (1.17e+7) —
		2.2392e+8 (1.16e+7) —	1.8848e+8 (5.79e+6) —	2.1511e+8 (7.43e+6) —	2.6475e+8 (9.09e+6) —	3.0163e+8 (1.02e+7) —	4.1221e+8 (1.12e+7) —	3.8121e+8 (1.44e+7) —
		2.0610e+8 (1.18e+7) —	1.8386e+8 (1.07e+7) —	1.9512e+8 (8.97e+6) —	2.1907e+8 (1.05e+7) —	2.7939e+8 (9.47e+6) —	3.8708e+8 (9.47e+6) —	3.5752e+8 (1.40e+7) —
		2.2542e+8 (8.65e+6) —	2.0746e+8 (6.13e+6) —	2.0389e+8 (6.29e+6) —	2.2737e+8 (1.87e+7) —	2.9682e+8 (1.53e+7) —	3.8475e+8 (1.48e+7) —	3.4562e+8 (1.59e+7) —
		2.8741e+8 (1.19e+7) —	2.1464e+8 (7.99e+6) —	2.8299e+8 (7.40e+6) —	2.8583e+8 (1.57e+7) —	3.5586e+8 (1.75e+7) —	4.4180e+8 (1.41e+7) —	4.2105e+8 (1.50e+7) —
		3.4231e+8 (7.76e+6) —	2.7942e+8 (1.02e+7) —	3.2372e+8 (8.94e+6) —	3.3118e+8 (1.36e+7) —	3.8673e+8 (1.07e+7) —	4.8172e+8 (9.82e+6) —	4.5895e+8 (1.17e+7) —
+ / - / ≈	vs MultiGPO2	0/9/0 1/7/1	0/9/0 0/9/0	0/9/0 1/8/1	0/9/0 0/9/0	0/9/0 0/9/0	0/9/0 0/9/0	0/8/1 8/0/1
WFG1 WFG2 WFG3 WFG4 WFG5 WFG6 WFG7 WFG8 WFG9	10	9.1173e+10 (6.62e+9) ≈	3.8066e+10 (4.59e+9) —	7.0210e+10 (8.37e+9) —	7.7758e+10 (1.38e+10) —	6.0453e+10 (1.06e+10) —	9.5114e+10 (1.07e+10) —	6.0375e+10 (9.54e+9) —
		7.0101e+10 (2.11e+10) —	4.9609e+10 (3.19e+9) —	6.7928e+10 (1.19e+10) —	7.0764e+10 (2.66e+9) —	6.3822e+10 (6.72e+9) —	8.7289e+10 (6.72e+9) —	6.7432e+10 (4.10e+9) —
		2.5546e+11 (2.63e+10) —	1.1414e+11 (9.44e+9) —	1.0571e+11 (1.97e+10) —	2.6028e+11 (1.56e+10) —	3.7485e+11 (1.23e+10) ≈	3.7668e+11 (2.09e+10) —	3.8661e+11 (1.57e+10) ≈
		2.9232e+11 (1.02e+10) —	1.4442e+11 (7.93e+9) —	2.8005e+11 (9.38e+9) —	2.7984e+11 (1.69e+10) —	2.7531e+11 (2.65e+10) —	5.9018e+11 (2.58e+10) —	3.1218e+11 (2.61e+10) —
		3.7973e+11 (1.14e+10) —	1.9422e+11 (8.22e+9) —	3.6578e+11 (1.46e+10) —	3.5504e+11 (1.06e+10) —	2.6626e+11 (1.83e+10) —	7.6289e+11 (3.03e+10) —	4.7701e+11 (2.84e+10) —
		2.7305e+11 (1.56e+10) —	1.6451e+11 (1.23e+10) —	2.6045e+11 (1.35e+10) —	2.2985e+11 (1.68e+10) —	1.6607e+11 (1.61e+10) —	5.8179e+11 (5.80e+10) —	2.9180e+11 (2.53e+10) —
		3.7695e+11 (3.90e+10) —	2.5391e+11 (1.27e+10) —	3.7916e+11 (2.03e+10) —	3.3081e+11 (1.65e+10) —	2.2464e+11 (2.30e+10) —	5.6030e+11 (2.83e+10) —	2.1260e+11 (2.13e+10) —
		3.8771e+11 (6.04e+10) —	1.7994e+11 (2.02e+10) —	3.6168e+11 (3.24e+10) —	2.5802e+11 (3.26e+10) —	2.6016e+11 (2.03e+10) —	7.8775e+11 (4.77e+10) —	5.6331e+11 (8.64e+10) —
		6.0477e+11 (5.15e+10) —	3.8472e+11 (2.36e+10) —	6.0275e+11 (2.28e+10) —	6.1281e+11 (3.40e+10) —	5.7458e+11 (2.14e+10) —	9.6462e+11 (3.73e+10) —	7.5333e+11 (2.82e+10) —
+ / - / ≈	vs MultiGPO2	0/8/1 2/6/1	0/9/0 1/8/0	0/9/0 2/6/1	0/9/0 3/6/0	0/8/1 0/7/2	0/8/1 8/0/1	0/8/1
WFG1 WFG2 WFG3 WFG4 WFG5 WFG6 WFG7 WFG8 WFG9	15	2.9951e+12 (2.55e+11) ≈	1.7735e+12 (2.24e+11) —	1.6683e+12 (3.97e+11) —	3.2114e+12 (4.24e+11) ≈	1.7417e+12 (2.79e+11) —	3.1990e+12 (3.52e+11) —	2.2926e+12 (4.84e+11) —
		3.4345e+12 (2.69e+11) ≈	1.0089e+12 (8.68e+10) —	1.5333e+12 (2.25e+11) —	2.6403e+12 (1.25e+11) —	2.2396e+12 (1.55e+11) —	3.3952e+12 (3.19e+11) —	2.6571e+12 (2.28e+11) —
		1.0090e+13 (2.46e+12) —	5.5994e+12 (6.55e+11) —	5.2840e+12 (8.36e+11) —	9.6709e+12 (8.20e+11) —	1.7911e+13 (1.23e+12) ≈	1.7377e+13 (1.34e+12) —	1.6885e+13 (1.47e+12) ≈
		2.3300e+13 (1.69e+12) —	8.2783e+12 (8.50e+11) —	2.2544e+13 (1.18e+12) —	9.7551e+12 (7.03e+11) —	5.2065e+12 (7.53e+11) —	2.5021e+13 (2.52e+12) —	1.4861e+13 (1.53e+12) —
		2.7686e+13 (2.11e+12) —	5.8348e+12 (7.30e+11) —	2.6525e+13 (1.07e+12) —	1.4737e+13 (8.07e+11) —	6.6077e+12 (1.14e+12) —	4.4970e+13 (2.36e+12) —	2.9400e+13 (1.55e+12) —
		2.4593e+13 (1.64e+12) ≈	4.6479e+12 (5.66e+11) —	2.3546e+13 (1.35e+12) —	8.8561e+12 (5.33e+11) —	2.9560e+12 (6.08e+11) —	2.4866e+13 (2.14e+12) —	1.0891e+13 (2.16e+12) —
		3.2265e+13 (2.68e+12) —	1.4607e+13 (1.46e+12) —	2.8834e+13 (7.76e+11) —	2.9156e+13 (3.66e+12) —	3.9740e+12 (1.25e+12) —	3.4991e+13 (2.51e+12) —	1.4320e+13 (2.72e+12) —
		2.5152e+13 (2.41e+12) —	5.7218e+12 (1.29e+12) —	2.1568e+13 (3.15e+12) —	1.6410e+13 (4.89e+12) —	8.0207e+12 (2.29e+12) —	2.7370e+13 (1.86e+12) —	2.3745e+13 (1.67e+12) —
		3.9928e+13 (3.50e+12) —	1.9249e+13 (3.19e+12) —	3.7676e+13 (1.49e+12) —	3.9614e+13 (4.37e+12) —	2.3869e+13 (2.07e+12) —	6.1038e+13 (2.74e+12) —	4.8092e+13 (2.37e+12) —
+ / - / ≈	vs MultiGPO2	0/6/3 6/3/0	0/9/0 0/8/1	0/9/0 3/6/0	0/8/1 2/6/1	0/8/1 1/8/0	0/8/1 8/0/1	0/8/1
Total (vs MultiGPO)		0/22/5	0/27/0	0/27/0	0/26/1	0/25/2		0/24/3
Total (vs MultiGPO2)		9/16/2	1/25/1	6/20/1	5/21/1	1/24/2	24/0/3	

TABLE S-IX

IGD RESULTS OF NSGA-III, MOEA/DD, θ -DEA, 1by1EA, NSGA-II/SDR, AND TWO MultiGPO ON MAF1–MAF15 WITH $G_{\max}=500$. THE BEST AND THE RESULT THAT IS STATISTICALLY SIMILAR TO THE BEST FOR EACH INSTANCE ARE SHOWN WITH DARK AND LIGHT GRAY BACKGROUND, RESPECTIVELY.

Problem	M	NSGA-III	MOEA/DD	θ -DEA	1by1EA	NSGA-II/SDR	MultiGPO	MultiGPO2
MaF1	5	1.8430e-1 (9.46e-3) —	2.1312e-1 (1.95e-2) —	2.1197e-1 (5.48e-3) —	1.0093e-1 (1.26e-3) +	1.0519e-1 (1.13e-3) +	1.0831e-1 (1.53e-3)	1.0766e-1 (1.51e-3) ≈
	8	2.3435e-1 (7.41e-3) —	3.5185e-1 (1.50e-2) —	2.6373e-1 (6.72e-3) —	2.2867e-1 (5.56e-2) ≈	1.8360e-1 (9.58e-4) +	1.9057e-1 (1.01e-3)	1.9063e-1 (1.42e-3) ≈
	10	4.7154e-1 (4.29e-2) —	4.7154e-1 (2.95e-2) —	3.1929e-1 (1.28e-2) —	3.1637e-1 (7.23e-2) —	2.1570e-1 (2.26e-3) —	2.3055e-1 (1.36e-3)	2.3035e-1 (1.80e-3) ≈
	15	3.2127e-1 (9.05e-3) —	5.3105e-1 (2.50e-2) —	3.3182e-1 (8.21e-3) —	4.5359e-1 (3.85e-2) —	2.8430e-1 (4.06e-3) +	3.0913e-1 (3.37e-3)	3.0811e-1 (2.73e-3) ≈
	20	3.1629e-1 (6.30e-3) —	6.3273e-1 (2.48e-2) —	2.7981e-1 (1.86e-2) —	5.8458e-1 (3.58e-2) —	3.4989e-1 (3.02e-3) +	4.0216e-1 (3.07e-3)	4.0172e-1 (2.31e-3) ≈
MaF2	5	1.1235e-1 (3.92e-3) —	1.2928e-1 (3.89e-3) —	1.2451e-1 (2.38e-3) —	8.2029e-2 (2.34e-3) +	9.5056e-2 (1.36e-3) +	9.6521e-2 (2.13e-3)	9.5547e-2 (1.65e-3) ≈
	8	1.9153e-1 (4.59e-2) —	1.8095e-1 (5.43e-3) —	1.6532e-1 (7.19e-3) —	2.0696e-1 (1.23e-2) —	1.8209e-1 (1.15e-2) —	1.4848e-1 (3.88e-3)	1.5000e-1 (4.39e-3) ≈
	10	2.0395e-1 (4.19e-2) —	2.5261e-1 (3.48e-2) —	2.0209e-1 (7.08e-3) —	2.7701e-1 (2.82e-2) —	2.2360e-1 (1.50e-2) —	1.8142e-1 (5.46e-3)	1.8808e-1 (1.06e-2) —
	15	2.0096e-1 (9.50e-3) ≈	4.2600e-1 (4.44e-2) —	2.8125e-1 (2.29e-2) —	4.8219e-1 (2.77e-2) —	3.4413e-1 (3.18e-2) —	2.0742e-1 (1.06e-2)	3.3336e-1 (2.98e-2) —
	20	3.1629e-1 (3.54e-2) —	4.6964e-1 (8.32e-2) —	2.7981e-1 (1.86e-2) —	5.7637e-1 (1.86e-2) —	3.5289e-1 (1.42e-2) —	2.0515e-1 (9.81e-3)	4.3535e-1 (4.32e-2) ≈
MaF3	5	7.4784e-2 (5.15e-3) +	9.5299e-2 (4.69e-3) +	9.8559e-2 (1.63e-3) +	1.5571e-1 (2.23e-2) —	1.4334e-1 (9.43e-3) —	1.1220e-1 (1.59e-2)	9.7021e-2 (1.28e-2) +
	8	1.2412e-1 (4.02e-1) ≈	1.1361e+0 (1.98e-0) ≈	1.2776e-1 (5.17e-3) —	1.4921e-1 (5.74e-3) —	1.7144e-1 (3.70e-3) —	1.1376e-1 (1.05e-2)	1.2453e-1 (1.69e-2) ≈
	10	4.8991e+1 (1.17e+3) +	1.0677e+0 (1.36e+0) +	1.5223e-1 (1.15e-1) +	1.5014e-1 (3.44e-3) +	1.8951e+3 (5.11e+3)	9.6858e+2 (2.34e+3) ≈	
	15	3.4740e-1 (4.74e-1) +	2.7003e+0 (6.93e-0) +	2.6075e-1 (8.70e-2) +	1.1608e+0 (2.81e+0) +	1.4077e-1 (1.90e-3) +	3.3831e+3 (9.17e+3)	6.0299e+3 (1.15e+4) ≈
	20	6.4860e+3 (1.25e+4) ≈	2.0256e+1 (2.79e+1) +	1.6490e+0 (4.34e+0) +	4.5744e+0 (1.48e+1) +	1.9825e-1 (1.08e-3) +	4.5087e+3 (4.76e+3)	3.5335e+3 (6.05e+3) ≈
MaF4	5	2.3764e-1 (1.92e-1) —	5.2811e+0 (6.02e-1) —	2.7721e+0 (2.34e-1) —	6.1418e+0 (6.37e-1) —	2.3533e+0 (1.87e-1) —	1.9223e+0 (4.67e-2)	2.3766e+0 (1.27e-1) —
	8	2.6603e+1 (1.58e+0) —	8.1206e+1 (4.32e+0) —	3.4357e+1 (2.31e+0) —	6.7292e+1 (7.46e+0) —	4.7764e+1 (8.17e+0) —	1.5974e+1 (7.92e-1)	1.8955e+1 (2.26e+0)
	10	9.8347e-1 (8.47e-0) —	3.9327e+0 (1.84e-1) —	1.2552e+0 (2.69e-1) —	2.8044e+2 (2.09e+1) —	1.8661e+2 (3.61e+1) —	6.0721e+1 (4.49e+0)	6.4479e+1 (5.20e+0) —
	15	3.9886e+3 (2.52e+2) +	1.5326e+4 (2.23e+3) +	4.4022e+2 (1.75e+2) +	9.9804e+3 (1.57e+3) +	7.7551e+3 (1.91e+3) +	1.7850e+3 (2.01e+2)	1.6628e+3 (1.67e+2) ≈
	20	1.2415e-1 (1.57e-1) —	5.5053e+0 (2.71e+0) —	1.6531e+1 (1.00e+0) —	3.7913e+5 (8.50e+3) —	2.8311e+5 (4.39e+4) —	5.5596e+4 (1.28e+4)	5.5133e+4 (1.15e+4) ≈
MaF5	5	1.9710e+0 (3.12e-3) —	3.8805e+0 (4.15e-1) —	1.9691e+0 (2.79e-3) —	3.7877e+0 (4.57e-1) —	1.2816e+1 (3.12e+0) —	1.9093e+0 (3.32e-2)	3.0327e+0 (3.35e-1) —
	8	1.9419e+1 (1.77e-1) +	7.6408e+1 (2.03e+0) +	1.9406e+1 (1.02e+1) +	4.8567e+1 (3.84e+0) +	8.3472e+1 (1.03e+1) +	3.2108e+1 (5.19e+0) +	2.7706e+1 (2.86e+0) +
	10	7.8045e-1 (6.39e-1) +	2.9042e+2 (1.23e+1) +	7.8028e+1 (8.39e-1) +	2.0342e+2 (1.14e+1) ≈	3.0086e+2 (2.41e+1) +	1.9561e+2 (2.73e+1) +	1.9217e+2 (2.19e+1) ≈
	15	2.4519e+3 (8.58e+1) +	7.3061e+3 (2.01e+1) +	2.4638e+3 (7.05e+1) +	5.9945e+3 (6.28e+1) +	7.3221e+3 (1.77e+1) +	6.0185e+3 (1.52e+1)	5.9343e+3 (4.23e+2) +
	20	7.0835e+3 (1.79e+4) +	1.7093e+4 (7.72e+4) +	7.0001e+4 (7.72e+4) +	1.4065e+5 (1.45e+3) +	1.6868e+5 (8.78e+3) +	1.3736e+5 (1.01e+4)	1.4046e+5 (5.32e+3) +
MaF6	5	1.6679e-1 (3.90e-3) —	6.7028e-2 (5.67e-3) —	8.6467e-2 (1.44e-2) —	2.1359e-3 (3.30e-5) +	1.3622e-2 (4.07e-3) —	3.3417e-3 (2.62e-4) +	2.8982e-3 (3.51e-4) +
	8	8.4718e-1 (1.34e-1) —	7.7435e-2 (3.52e-3) —	7.9149e-2 (3.87e-2) —	1.8380e-3 (2.53e-5) +	1.4313e-2 (2.6e-3) —	2.7859e-3 (2.70e-4) —	3.5835e-3 (5.65e-4) —
	10	3.9549e-1 (1.60e-1) —	9.7140e-2 (6.95e-3) —	1.3072e-1 (2.10e-1) —	1.6040e-3 (1.60e-5) +	7.3893e-3 (2.74e-3) +	8.4012e-2 (1.49e-1)	1.9895e-1 (2.04e-1)
	15	4.9828e-1 (1.73e-1) ≈	1.3028e-1 (4.37e-3) +	3.7881e-1 (1.33e-2) +	1.8422e-1 (2.91e-5) +	3.7630e-2 (8.68e-2) +	4.5053e-1 (1.72e-1)	4.4088e-1 (1.10e-1) ≈
	20	6.8659e+0 (2.86e+0) —	1.6937e-1 (2.59e-2) —	5.51542e-1 (2.13e-1) ≈	2.1043e-3 (3.95e-5) +	8.3904e-2 (1.20e-1) +	4.4574e-1 (1.03e-1)	4.9918e-1 (1.70e-1) ≈
MaF7	5	2.9292e-1 (8.23e-3) —	2.77112e-0 (7.06e-1) —	2.9729e-1 (2.21e-2) —	3.0631e-1 (2.86e-2) —	3.2319e-1 (3.17e-2) —	2.8153e-1 (1.08e-1) —	2.9581e-1 (1.93e-1) ≈
	8	6.7268e-1 (9.88e-3) —	1.7948e+0 (5.15e-1) —	7.8332e-1 (8.00e-2) —	1.1247e+0 (1.02e-1) —	8.5172e-1 (6.61e-2) —	5.5177e-1 (1.90e-1) +	
	10	1.0626e+0 (1.04e-1) —	2.2466e+0 (4.48e-1) —	9.6154e-1 (1.38e-1) ≈	2.2580e+0 (4.13e-1) —	1.6365e+0 (3.00e-1) —	8.9535e-1 (1.86e-1)	8.3376e-1 (6.77e-3) +
	15	4.9000e+0 (1.13e+0) —	3.4175e+0 (3.61e-2) —	9.3193e+0 (8.04e-1) —	3.2753e+0 (3.95e-1) —	4.0091e+1 (5.84e-1) —	2.0198e+0 (1.89e-1)	1.7227e+0 (1.11e-1) +
	20	9.3379e+0 (1.32e+0) —	1.5801e+1 (0.97e+0) —	9.4833e+0 (1.29e+0) —	3.6358e+0 (2.35e-1) —	7.1990e+0 (8.40e-1) —	4.5088e+0 (1.18e+0)	2.1397e+0 (1.81e+1) —
MaF8	5	1.6465e-1 (1.06e-2) —	2.8093e-1 (2.07e-2) —	2.9654e-1 (3.39e-2) —	3.8350e-1 (6.36e-2) —	1.0296e-1 (6.15e-3) —	7.7241e-2 (9.52e-4) —	7.4496e-2 (1.05e-3) +
	8	2.9912e-1 (1.67e-2) —	5.5649e-1 (3.89e-2) —	5.8117e-1 (8.38e-2) —	3.6331e-1 (1.64e-2) —	1.3645e-1 (1.01e-2)	9.8425e-2 (1.31e-3) —	1.0032e-1 (1.46e-3)
	10	3.1862e-1 (6.01e-2) —	9.0495e-1 (2.87e-2) —	7.0454e-1 (1.08e-1) —	3.2885e-1 (6.56e-2) —	1.4361e-1 (9.62e-3) —	1.0283e-1 (1.13e-3)	1.3703e-1 (5.48e-3) —
	15	3.7467e-1 (6.74e-2) —	1.3245e+0 (3.65e-2) —	9.4622e-1 (1.18e-1) —	4.0811e-1 (8.01e-2) —	2.0206e-1 (1.60e-2)	1.3727e-1 (1.70e-3)	1.9285e-1 (7.74e-3)
	20	20.4136e-1 (6.53e-2) —	1.8218e+0 (1.12e-1) —	9.8724e-1 (9.53e-2) —	4.7151e-1 (1.55e-2) —	2.7186e-1 (3.08e-2) —	1.7373e-1 (2.37e-3)	2.2721e-1 (1.97e-3) —
MaF9	5	4.5167e-1 (1.86e-1) —	2.2621e-1 (3.82e-3) —	7.0039e-1 (1.61e-1) —	1.5417e-1 (5.59e-2) —	1.3686e-1 (3.76e-3) —	7.1828e-2 (5.99e-4) —	7.1440e-2 (6.01e-4) ≈
	8	1.1130e-1 (0.13e+0) —	4.5976e-1 (4.21e-1) —	9.2180e-1 (1.24e-1) —	1.2473e-1 (5.55e-2) —	1.6804e-1 (8.50e-3) —	9.1333e-2 (5.20e-4) —	9.1594e-2 (5.42e-4) ≈
	10	5.2409e-1 (1.07e-1) —	5.9439e-1 (2.82e-3) —	7.8851e-1 (1.18e-1) —	1.1228e-1 (7.73e-3) —	1.7150e-1 (1.23e-2) —	9.7460e-2 (7.53e-4) —	
	15	4.5779e-1 (3.99e-1) —	9.5655e-1 (1.65e-2) —	1.5303e+0 (2.44e+0) —	2.1753e-1 (1.78e-1) —	1.9124e-1 (7.42e-3) —	1.3070e-1 (8.13e-1) —	
	20	6.1695e+0 (7.60e+0) —	2.5832e+0 (3.62e+0) —	8.3611e+0 (7.92e+0) —	3.5676e-1 (1.29e-1) —	2.3087e-1 (4.98e-3) —	1.6364e-1 (5.45e-3)	1.6280e-1 (3.42e-3) ≈
MaF10	5	4.9768e-1 (4.57e-2) ≈	6.1549e-1 (4.21e-2) —	4.0070e-1 (2.29e-2) —	7.0216e-1 (6.47e-2) —	6.3777e-1 (7.42e-2) —	5.1489e-1 (6.97e-2) —	5.6662e-1 (2.01e-1) ≈
	8	1.0574e-0 (9.68e-2) —	1.3770e+0 (1.14e-1) —	8.5924e-1 (4.25e-2) —	1.7123e+0 (7.23e-2) —	1.6562e+0 (6.63e-1) —	8.7875e-1 (4.33e-2) —	1.2289e+0 (2.41e-1) —
	10	1.1984e-0 (5.05e-2) —	1.2725e+0 (7.61e-2) —	9.8461e-1 (2.90e-2) —	1.8980e+0 (4.03e-2) —	1.7890e+0 (7.14e-2) —	1.1042e+0 (1.32e-1)	1.5823e+0 (7.53e-2) —
	15	1.8022e+0 (7.53e-2) ≈	2.0663e+0 (5.39e-2) +	1.5233e+0 (2.05e-2) +	2.4545e+0 (1.95e-2) —	2.4549e+0 (6.89e-2) +	1.7975e+0 (1.09e-1) —	2.2215e+0 (1.85e-1) —
	20	4.5157e+0 (2.31e-1) —	5.2421e+0 (1.26e-2) —	3.9862e+0 (4.37e-1) ≈	5.2060e+0 (1.53e-2) —	5.1418e+0 (4.19e-2) —	3.9733e+0 (3.63e-1) —	3.8647e+0 (4.17e-1) ≈
MaF11	5	5.8850e-1 (1.89e-3) +	5.0532e-1 (1.51e-2) —	3.8911e-1 (2.42e-2) —	6.4773e-1 (6.20e-2) —	4.9884e-1 (4.79e-2) —	4.8300e-1 (1.34e-1) —	7.0319e-1 (1.38e-1) —
	8	9.5469e-1 (1.86e-1) —	1.1879e+0 (1.90e-2) +	9.3293e-1 (1.222e-1) +	1.6981e+0 (6.22e-2) —	1.3920e+0 (4.14e-1) —	1.2403e+0 (8.85e-2) —	1.7095e+0 (1.36e-1) —
	10	1.1710e+0 (1.76e-1) +	1.4487e+0 (2.18e-2) —	1.1471e+0 (7.34e-2) +	1.8385e+0 (3.18e-2) —	1.6419e+0 (1.39e-1) —	1.4740e+0 (6.72e-2) —	1.9470e+0 (5.64e-2) —
	15	1.6116e+0 (7.48e-2) —	1.8908e+0 (4.86e-2) —	3.7522e+0 (1.51e+0) —	2.3920e+0 (7.00e-2) —	2.3511e+0 (7.18e-2) —	2.2008e+0 (1.05e-1)	2.4566e+0 (1.60e-1)
	20	2.4526e+0 (1.13e+0) +	5.5434e+0 (1.04e-2) —	4.4022e+0 (4.09e-1) ≈	4.9681e+0 (1.55e-1) —	5.1930e+0 (1.16e-1) —	4.5468e+0 (1.63e-1)	5.0468e+0 (1.45e-1)
MaF12	5	9.3372e-1 (3.30e-3) —	1.0348e+0 (5.74e-3) —	9.3372e-1 (3.17e-3) —	1.3826e+0 (9.95e-2) —	9.7747e-1 (1.08e-2) —	9.2423e-1 (5.68e-3)	9.4444e-1 (1.58e-2) —
	8	2.7735e-0 (5.15e-2) —	3.2685e-0 (6.67e-2) —	2.7597e-0 (6.61e-2) ≈	3.8291e-0 (1.99e-1) —	2.8849e-0 (1.26e-2) —	2.7549e-0 (2.49e-2) —	2.7435e-0 (2.30e-2) ≈
	10	4.3981e+0 (3.15e-2) —	6.0534e+0 (2.28e-1) —	4.3791e-0 (2.89e-2) —	5.5274e-0 (2.33e-1) —	4.3333e-0 (4.07e-2) —	3.9834	

TABLE S-X

HV RESULTS OF NSGA-III, MOEA/DD, θ -DEA, 1BY1EA, NSGA-II/SDR, AND TWO MultiGPO ON MAF1–MAF15 WITH $G_{\max}=500$. THE BEST AND THE RESULT THAT IS STATISTICALLY SIMILAR TO THE BEST FOR EACH INSTANCE ARE SHOWN WITH DARK AND LIGHT GRAY BACKGROUND, RESPECTIVELY.

Problem	M	NSGA-III	MOEA/DD	θ DEA	1by1EA	NSGA-II/SDR	MultiGPO	MultiGPO2
MaF1	5	6.5643e-3 (5.17e-4) —	5.6372e-3 (4.54e-4) —	5.6231e-3 (1.42e-4) —	1.3311e-2 (0.987e-5) +	1.3002e-2 (1.35e-4) +	1.1715e-2 (2.74e-4) —	1.1960e-2 (2.20e-4)
	8	3.0700e-5 (1.83e-6) ≈	1.2188e-5 (2.19e-6) —	2.9017e-5 (1.41e-6) ≈	3.7482e-5 (1.32e-5) ≈	4.1304e-5 (2.68e-6) +	3.0951e-5 (6.70e-6) ≈	3.1990e-5 (6.37e-6)
	10	4.5207e-7 (2.30e-8) ≈	3.6154e-8 (1.17e-8) —	3.3542e-7 (4.95e-8) ≈	3.5763e-7 (2.26e-7) ≈	3.5763e-7 (4.54e-7) ≈	2.8866e-7 (4.54e-7) ≈	3.4713e-7 (4.85e-7)
MaF2	5	1.8798e-1 (1.69e-3) ≈	1.5757e-1 (3.63e-3) —	1.7346e-1 (3.23e-3) —	1.8845e-1 (2.05e-3) ≈	2.0296e-1 (1.40e-3) +	1.8604e-1 (3.35e-3) ≈	1.8799e-1 (2.45e-3)
	8	1.5128e-1 (6.84e-3) —	1.5882e-1 (3.83e-3) —	1.8207e-1 (8.01e-3) —	2.1655e-1 (3.10e-3) —	2.3236e-1 (2.25e-3) +	2.2030e-1 (3.72e-3) —	2.2359e-1 (2.48e-3)
	10	2.1627e-1 (5.55e-3) —	1.8250e-1 (5.60e-3) —	1.9630e-1 (7.31e-3) —	2.0124e-1 (5.05e-3) —	2.2329e-1 (2.79e-3) —	2.0997e-1 (5.81e-3) —	2.2638e-1 (2.90e-3)
MaF3	15	1.3590e-1 (1.45e-2) —	9.4247e-2 (3.47e-3) —	1.2429e-1 (1.25e-2) —	1.8056e-1 (5.12e-3) —	2.0632e-1 (6.73e-3) —	1.7052e-1 (4.54e-3) —	2.1584e-1 (3.36e-3)
	20	1.2277e-1 (2.12e-2) —	1.4378e-1 (8.18e-3) —	1.7813e-1 (2.47e-3) —	1.6563e-1 (6.99e-3) —	2.1778e-1 (2.88e-3) +	1.4755e-1 (5.79e-3) —	2.1219e-1 (2.79e-3)
	5	9.9889e-1 (4.92e-4) ≈	9.9162e-1 (2.90e-3) —	9.9199e-1 (1.67e-3) —	9.8319e-1 (1.78e-2) —	9.8200e-1 (5.36e-3) —	9.9678e-1 (2.19e-3) +	9.9967e-1 (2.11e-3)
MaF4	8	5.9982e-1 (5.07e-1) ≈	6.6580e-1 (1.30e-1) —	9.9710e-1 (1.86e-3) —	9.9906e-1 (4.79e-4) ≈	9.9213e-1 (2.75e-3) —	9.9996e-1 (4.23e-5) +	9.9886e-1 (1.29e-3)
	10	9.9984e-2 (3.08e-1) ≈	5.4212e-1 (4.33e-1) ≈	9.4147e-1 (8.00e-2) +	9.7979e-1 (6.97e-2) +	9.9288e-1 (2.33e-3) +	5.0000e-2 (2.24e-1) —	2.7694e-1 (4.36e-1)
	15	9.1095e-2 (2.58e-1) ≈	5.9098e-2 (1.20e-1) +	9.1622e-1 (7.54e-2) +	7.4799e-1 (4.15e-1) +	9.9526e-1 (1.42e-3) +	0.00e+0 (0.00e+0) ≈	0.00e+0 (0.00e+0)
MaF5	20	0.00e+0 (0.00e+0) ≈	5.7254e-3 (1.53e-2) ≈	7.1970e-1 (3.81e-1) +	7.2791e-1 (4.45e-1) +	9.9652e-1 (1.07e-3) +	0.00e+0 (0.00e+0) ≈	0.00e+0 (0.00e+0)
	5	5.7578e-2 (5.51e-3) —	5.1321e-2 (6.26e-3) —	8.1565e-2 (1.15e-2) —	7.1778e-2 (1.16e-2) —	1.3139e-1 (1.31e-3) +	1.1965e-1 (2.84e-3) +	1.1172e-1 (5.31e-3)
	8	1.9658e-3 (1.92e-4) ≈	2.4531e-5 (1.23e-5) —	1.1795e-3 (3.53e-4) —	1.9503e-4 (6.98e-5) —	7.0521e-4 (1.70e-4) —	2.7156e-3 (2.53e-4) +	2.0274e-3 (1.83e-4)
MaF6	10	2.2631e-4 (2.38e-5) +	1.3158e-7 (2.86e-8) —	2.0254e-4 (3.14e-5) +	2.3443e-6 (1.94e-6) —	1.5104e-5 (2.83e-6) —	1.1167e-4 (1.84e-5) +	8.4665e-5 (1.35e-5)
	15	1.9430e-7 (2.67e-8) +	5.532e-13 (1.90e-13) —	1.614e-7 (2.26e-8) —	9.510e-12 (1.46e-11) —	2.274e-10 (1.89e-10) —	4.1732e-9 (1.08e-8) ≈	3.9886e-9 (1.23e-8)
	20	1.07e-10 (2.99e-11) +	2.01e-18 (5.13e-19) +	1.37e-10 (9.79e-12) +	1.29e-17 (1.48e-17) +	2.23e-15 (2.43e-15) +	0.00e+0 (0.00e+0) ≈	0.00e+0 (0.00e+0)
MaF7	5	8.1219e-1 (4.74e-4) +	6.8268e-2 (1.17e-2) —	8.1238e-1 (3.85e-4) +	6.7739e-1 (1.08e-2) —	1.8801e-1 (1.52e-1) —	8.0359e-1 (2.28e-3) +	7.6757e-1 (1.06e-2)
	8	9.4465e-1 (5.21e-4) +	8.9238e-3 (4.83e-3) —	9.2603e-1 (2.95e-4) —	7.6045e-1 (1.59e-2) —	1.1186e-1 (3.64e-2) —	8.8610e-1 (6.04e-3) ≈	8.8226e-1 (8.76e-3)
	10	9.6951e-1 (2.07e-4) +	5.8461e-1 (1.90e-2) —	9.6994e-1 (2.20e-4) +	8.0673e-1 (1.09e-2) —	1.0455e-1 (3.70e-2) —	9.0370e-1 (6.16e-3) —	9.1223e-1 (7.18e-3)
MaF8	15	9.9090e-1 (1.34e-4) +	4.8542e-1 (2.63e-2) —	9.9127e-1 (9.10e-5) +	8.6741e-1 (1.16e-2) —	1.0472e-1 (4.24e-2) —	9.4939e-1 (5.60e-3) +	9.4366e-1 (5.63e-3)
	20	9.8872e-1 (1.41e-2) +	4.4241e-1 (3.96e-2) +	9.9865e-1 (3.58e-5) +	9.0554e-1 (8.47e-3) —	1.0575e-1 (3.71e-2) —	9.6699e-1 (3.56e-3) +	9.5989e-1 (4.10e-3)
	5	1.2374e-1 (1.59e-3) —	1.1594e-1 (7.45e-4) —	1.1617e-1 (1.42e-3) —	1.2959e-1 (3.02e-4) +	1.2437e-1 (2.66e-3) —	1.2999e-1 (3.44e-4) +	1.2904e-1 (5.02e-4)
MaF9	8	8.8085e-2 (3.04e-2) —	9.6397e-2 (6.69e-4) —	1.0297e-1 (3.98e-4) —	1.0641e-1 (3.14e-2) +	1.0379e-1 (1.35e-3) —	1.0609e-1 (3.02e-4) +	1.0536e-1 (3.28e-4)
	10	9.1795e-1 (5.75e-3) +	9.4209e-2 (9.67e-4) ≈	8.2145e-2 (3.32e-2) ≈	1.0093e-1 (3.58e-4) +	9.9875e-2 (6.32e-4) +	8.0966e-2 (3.72e-2) +	6.1217e-2 (4.33e-2)
	15	9.5542e-3 (2.35e-2) ≈	9.2299e-2 (4.31e-4) +	1.6542e-2 (3.48e-2) +	9.5279e-2 (2.68e-4) +	9.4400e-2 (1.26e-3) +	9.0926e-3 (1.89e-2) ≈	1.1206e-2 (2.20e-2)
MaF10	20	0.00e+0 (0.00e+0) —	9.1097e-2 (4.07e-4) +	2.081e-3 (5.88e-3) —	9.3278e-2 (2.72e-4) +	9.2308e-2 (9.61e-4) +	8.4863e-3 (1.64e-2) ≈	6.3601e-3 (1.77e-2)
	5	2.5778e-1 (3.40e-3) —	9.6008e-2 (1.57e-2) —	2.2013e-1 (1.07e-2) —	1.9595e-2 (1.57e-2) —	2.5817e-1 (2.15e-3) —	2.4889e-1 (4.10e-3) —	2.5997e-1 (1.16e-2)
	8	2.0682e-1 (2.50e-3) +	3.1157e-2 (2.69e-2) —	1.8497e-1 (2.20e-2) +	8.4737e-2 (1.43e-2) —	2.0215e-2 (1.45e-3) +	1.3835e-1 (1.54e-2) ≈	1.3665e-1 (2.83e-2)
MaF11	10	1.7143e-1 (2.13e-2) +	1.7515e-3 (7.52e-3) —	1.8678e-1 (8.03e-3) —	6.1121e-2 (1.31e-2) —	1.6638e-1 (4.35e-3) +	9.9000e-2 (2.11e-2) ≈	9.4034e-2 (2.38e-2)
	15	7.1235e-2 (2.09e-2) ≈	3.7964e-2 (7.20e-8) +	9.3995e-2 (2.37e-2) +	6.4232e-4 (1.97e-3) —	2.5450e-3 (1.00e-2) —	7.6380e-2 (2.27e-2) ≈	6.1721e-2 (2.79e-2)
	20	0.00e+0 (0.00e+0) —	7.1874e-18 (2.63e-17) —	1.3782e-1 (7.32e-3) +	2.9982e-9 (5.85e-9) —	0.00e+0 (0.00e+0) —	9.3477e-2 (2.08e-2) +	3.8946e-2 (2.08e-2)
MaF12	5	1.0817e-1 (2.35e-3) —	8.2053e-2 (4.59e-3) —	8.5118e-2 (5.57e-3) —	9.9937e-2 (6.95e-3) —	1.2338e-1 (5.55e-4) —	1.2599e-1 (4.03e-4) —	1.2647e-1 (4.21e-4)
	8	6.4452e-2 (7.80e-4) —	1.8871e-2 (1.71e-3) —	1.7385e-2 (2.79e-3) —	2.9923e-2 (9.70e-4) —	3.1411e-2 (1.74e-4) —	3.1803e-2 (2.30e-4) —	3.2087e-2 (9.81e-5)
	10	9.3073e-3 (2.65e-4) —	6.0055e-3 (2.06e-4) —	5.9354e-3 (6.86e-4) —	1.1014e-2 (2.05e-4) —	1.0946e-2 (9.54e-5) —	1.1045e-2 (1.02e-4) —	1.1206e-2 (5.81e-5)
MaF13	15	5.1403e-4 (2.85e-5) —	3.1342e-4 (1.32e-5) —	3.0900e-4 (5.26e-5) —	6.6231e-4 (6.69e-6) ≈	6.2141e-4 (9.36e-6) —	6.2072e-4 (2.25e-5) —	6.6016e-4 (1.27e-5)
	20	1.0819e-5 (3.74e-5) +	1.8091e-5 (3.31e-6) +	5.1074e-5 (3.16e-6) +	3.9347e-5 (3.52e-6) +	3.5372e-5 (2.15e-6) +	3.6199e-5 (5.09e-6) ≈	3.9422e-5 (1.03e-6)
	5	1.9338e-1 (5.11e-2) —	2.5173e-1 (2.01e-3) —	1.2533e-1 (3.97e-2) —	2.7564e-1 (2.46e-2) —	2.9034e-1 (3.82e-3) —	3.2608e-1 (6.40e-4) ≈	3.2653e-1 (9.57e-4)
MaF14	8	2.2327e-2 (1.53e-2) —	2.2812e-2 (1.65e-2) —	2.3235e-2 (1.16e-2) —	5.1313e-1 (3.78e-4) —	4.5157e-2 (6.21e-4) —	5.2864e-2 (2.31e-4) —	5.3019e-2 (1.71e-4)
	10	9.1037e-1 (6.51e-2) —	9.8755e-1 (1.97e-2) —	9.9562e-1 (1.18e-3) —	1.8414e-2 (3.54e-4) —	1.6025e-2 (4.17e-4) —	1.8812e-2 (1.65e-4) ≈	1.8829e-2 (1.41e-4)
	15	9.8771e-1 (3.17e-2) —	9.8018e-1 (5.02e-2) —	9.9722e-1 (6.22e-2) —	9.9788e-1 (2.24e-4) —	9.8025e-1 (2.09e-2) —	9.9843e-1 (6.95e-4) ≈	9.9858e-1 (4.34e-4)
MaF15	20	9.9873e-1 (7.98e-4) ≈	9.7721e-1 (4.63e-3) —	9.9903e-1 (7.25e-4) —	9.9879e-1 (1.81e-4) —	9.9219e-1 (6.13e-3) —	9.9851e-1 (7.25e-4) —	9.9804e-1 (7.48e-4)
	5	9.9388e-1 (1.09e-3) +	9.7476e-1 (4.17e-3) —	9.9340e-1 (9.91e-4) +	9.7959e-1 (3.44e-3) —	9.7419e-1 (5.19e-3) —	9.8523e-1 (1.51e-3) +	9.8384e-1 (1.91e-3)
	8	9.9312e-1 (2.78e-3) +	9.6798e-1 (1.98e-3) —	9.9033e-1 (2.37e-3) ≈	9.9090e-1 (2.66e-3) —	9.7963e-1 (5.29e-3) —	9.9110e-1 (2.10e-3) ≈	9.9054e-1 (2.19e-3)
MaF16	10	9.9511e-1 (2.95e-3) +	9.5890e-1 (5.44e-4) +	9.9000e-1 (3.05e-3) +	9.9261e-1 (2.01e-3) +	9.8643e-1 (3.14e-3) ≈	9.9398e-1 (1.11e-3) +	9.8810e-1 (2.67e-3)
	15	9.9163e-1 (2.63e-3) ≈	9.7489e-1 (9.50e-3) +	9.2900e-1 (7.21e-2) +	9.9284e-1 (8.48e-4) +	9.8950e-1 (2.46e-3) —	9.9374e-1 (1.62e-3) ≈	9.9450e-1 (4.89e-3)
	20	9.7874e-1 (4.66e-2) —	9.3176e-1 (6.70e-3) —	9.6634e-1 (1.16e-2) —	9.9105e-1 (3.50e-3) —	9.8893e-1 (1.95e-3) —	9.9334e-1 (3.13e-3) ≈	9.9450e-1 (4.33e-3)
MaF17	5	5.7439e-1 (5.44e-3) +	7.1770e-1 (1.15e-2) —	7.6275e-1 (4.67e-3) +	6.4812e-1 (1.25e-2) —	7.6103e-1 (4.47e-3) +	7.2755e-1 (5.88e-3) —	7.4560e-1 (6.67e-3)
	8	7.9494e-1 (5.18e-2) —	7.2949e-1 (2.47e-2) —	8.2707e-1 (3.37e-2) —	7.1752e-1 (3.99e-2) —	8.7602e-1 (2.95e-3) +	8.0378e-1 (7.46e-3) —	8.5401e-1 (5.09e-3)
	10	8.6521e-1 (4.68e-2) —	6.5049e-1 (4.46e-2) —	8.8430e-1 (9.26e-3) —	7.4913e-1 (3.73e-2) —	9.0789e-1 (3.89e-3) +	8.3036e-1 (8.54e-3) —	8.8527e-1 (4.15e-2)
MaF18	15	8.6939e-1 (6.01e-2) ≈	6.4942e-1 (8.34e-2) —	8.4710e-1 (1.02e-2) —	7.4935e-1 (4.42e-2) —	9.1962e-1 (3.90e-2) —	8.1253e-1 (3.90e-2) —	8.8256e-1 (4.30e-2)
	20	8.0404e-1 (4.86e-2) —	5.2952e-1 (3.23e-1) —	9.0128e-1 (1.18e-2) —	7.3043e-1 (4.94e-2) —	8.8461e-1 (7.28e-2) ≈	8.1290e-1 (2.32e-2) —	9.1080e-1 (1.43e-2)
	5	2.1002e-1 (1.81e-2) —	2.3501e-1 (1.33e-2) —	1.4409e-1 (3.73e-2) —	2.9432e-1 (3.31e-3) —	2.5149e-1 (6.05e-3) —	2.7745e-1 (8.43e-3) ≈	2.7297e-1 (1.15e-2)
MaF19	8	1.2007e-1 (2.18e-2) —	7.0533e-2 (7.89e-3) —	1.3072e-2 (1.78e-2) —	1.8072e-1 (1.70e-3) —	1.4890e-1 (5.54e-3) —	1.6577e-1 (6.33e-3) ≈	1.6159e-1 (5.30e-3)
	10	9.3372e-2 (1.91e-2) —	5.0469e-2 (1.23e-2) —	4.4330e-3 (8.24e-3) —	1.4553e-1 (1.06e-3) —	1.1636e-1 (4.65e-3) —	1.2974e-1 (5.90e-3) ≈	1.3206e-1 (2.11e-3)
	15	5.8873e-2 (1.68e-2) —	3.0432e-2 (1.25e-2) —	7.0181e-2 (8.82e-5) —	9.4000e-2 (8.48e-4) —	7.5268e-2 (4.76e-3) —	8.5579e-2 (3.59e-3) —	8.6815e-2 (1.82e-3)
MaF20</								

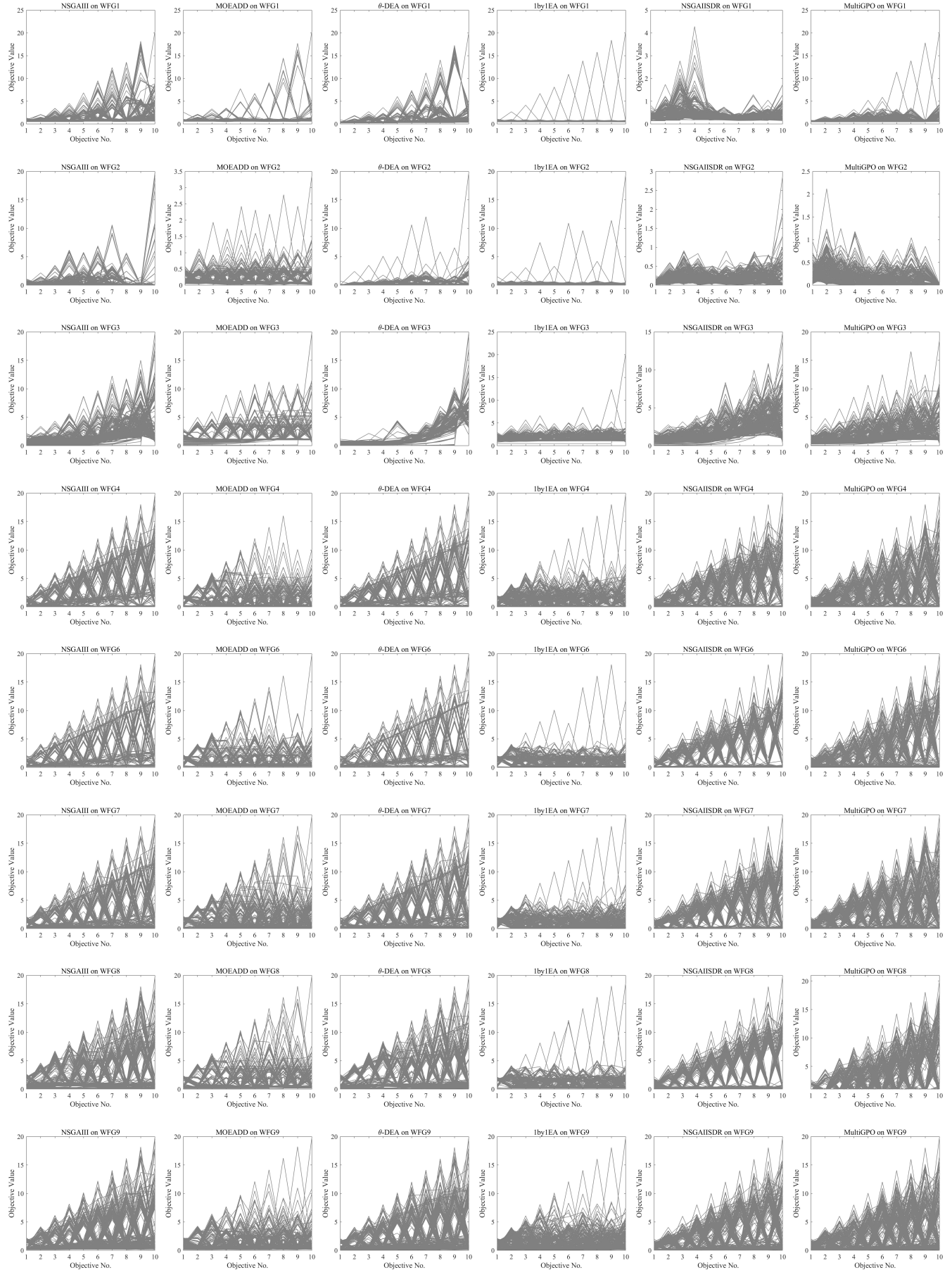


Fig. S-10. Parallel coordinates of the objective values for each algorithm on ten-objective WFG.

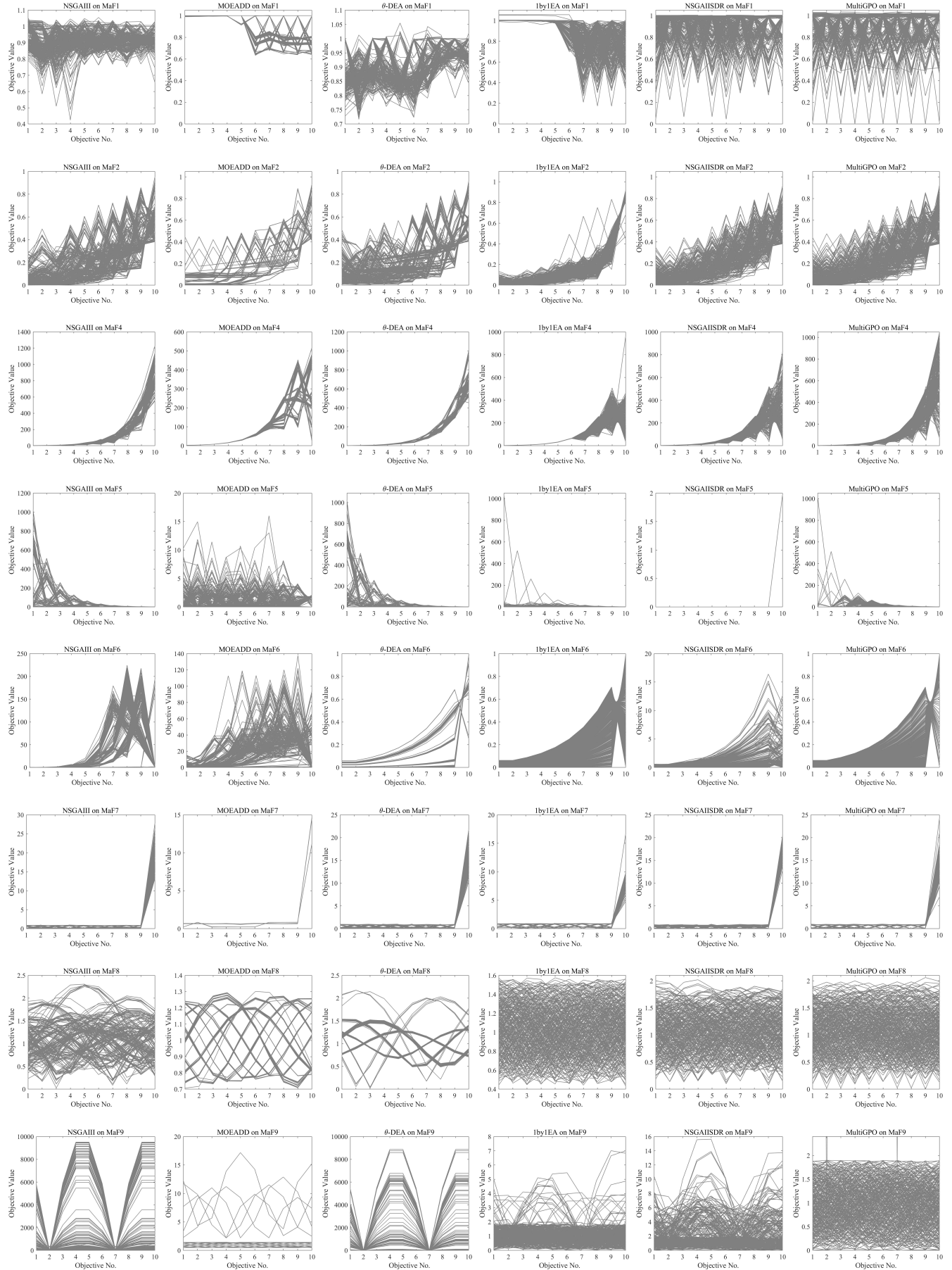


Fig. S-11. Parallel coordinates of the objective values for each algorithm on ten-objective MaF.

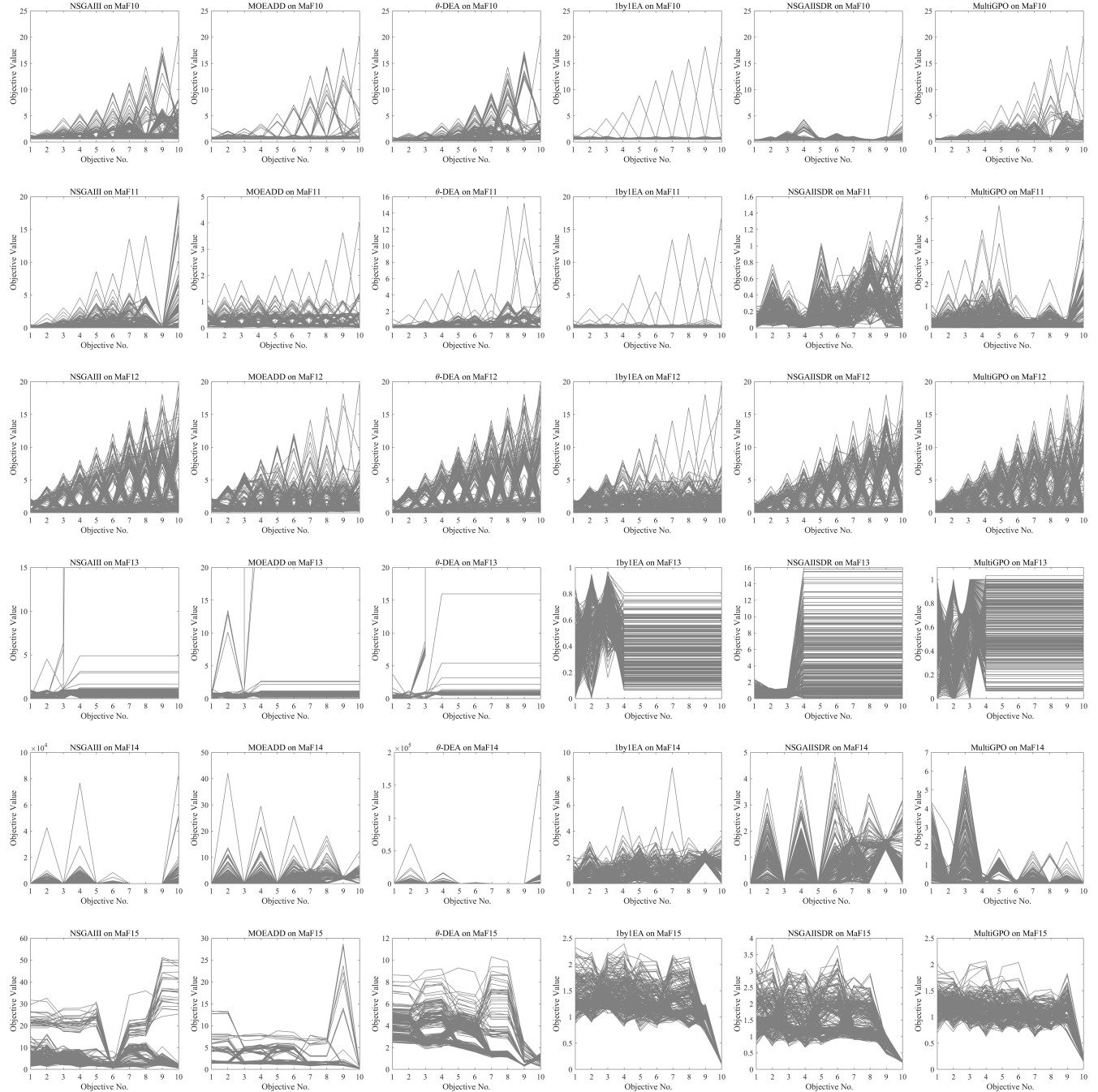


Fig. S-12. Parallel coordinates of the objective values for each algorithm on ten-objective MaF.

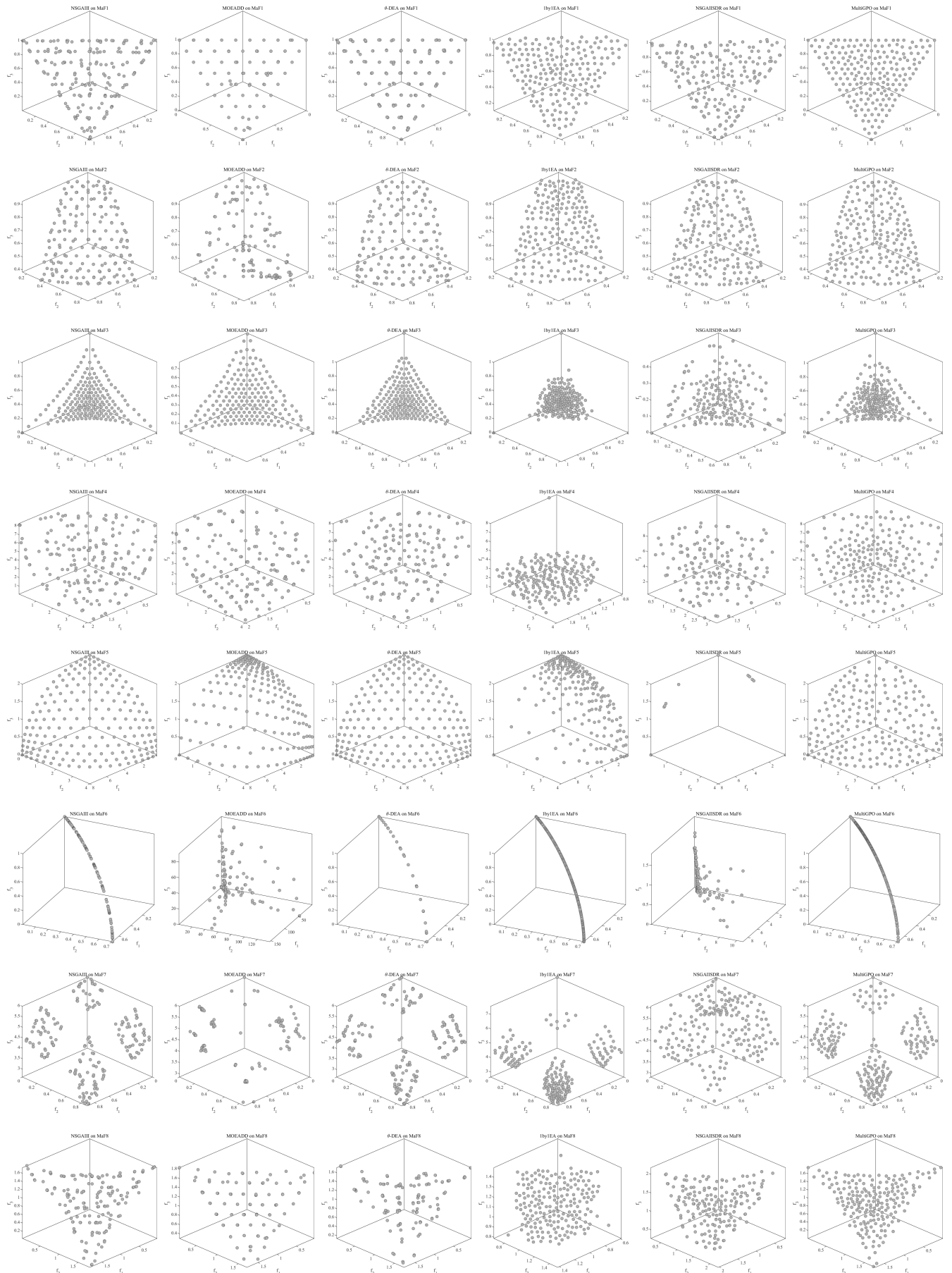


Fig. S-13. Plot results for each algorithm on three-objective MaF.

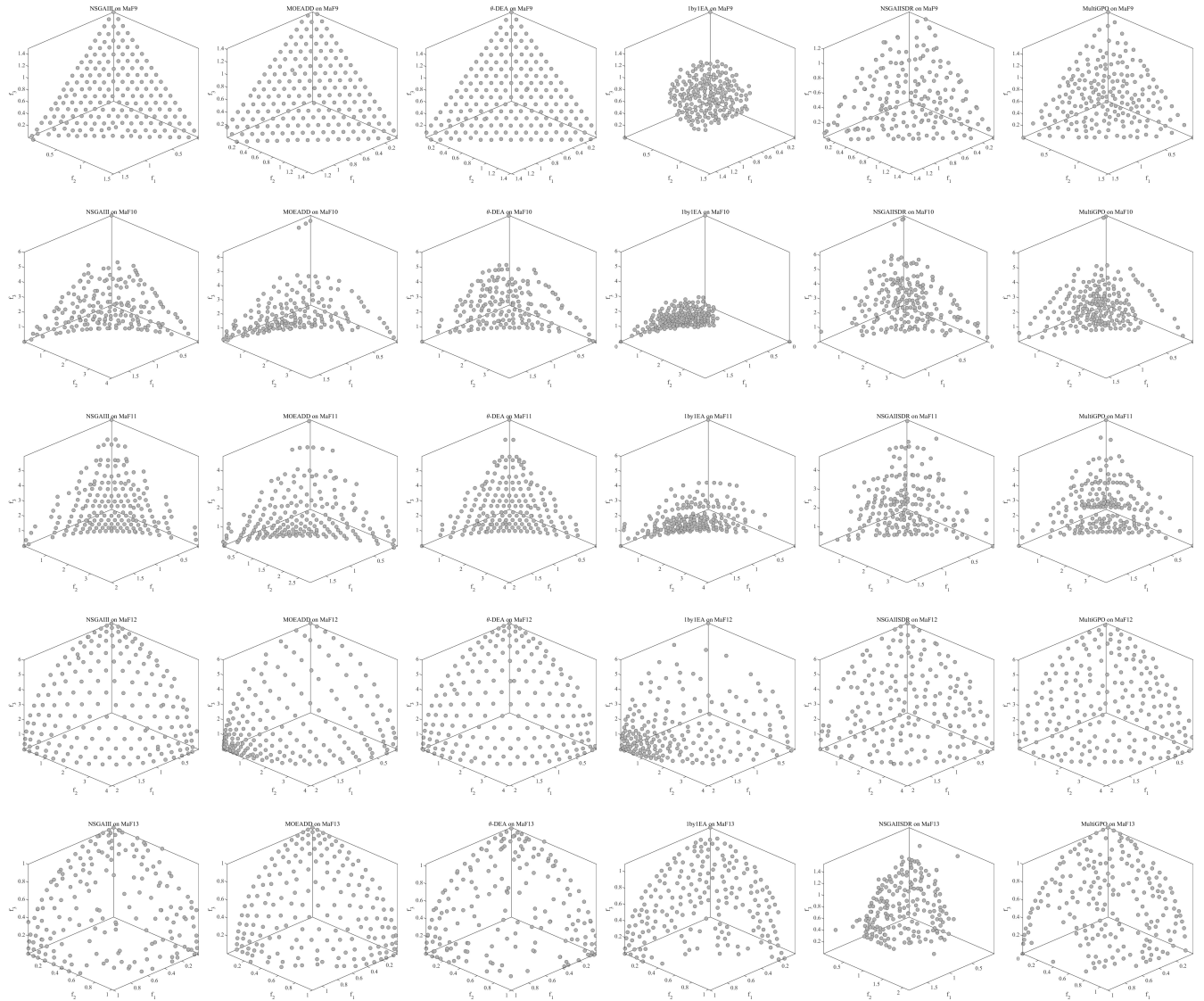


Fig. S-14. Plot results for each algorithm on three-objective MaF.

TABLE S-XI
IGD RESULTS OF ALL METHODS ON MAF1-MAF15 WITH $G_{\max}=200$.

Problem	M	NSGA-III	MOEA/DD	θ -DEA	IbyIEA	NSGA-II/SDR	MultiGPO	MultiGPO2
MaF1	5	1.8383e-1 (8.67e-3) —	2.0847e-1 (1.36e-3) —	2.0856e-1 (1.21e-2) —	1.0176e-1 (2.76e-3) +	1.0473e-1 (1.12e-3) +	1.0882e-1 (1.39e-3)	1.0745e-1 (1.20e-3) +
	8	2.3688e-1 (7.06e-3) —	3.6135e-1 (1.92e-2) —	2.6139e-1 (1.06e-2) —	3.6591e-1 (3.36e-2) —	1.8480e-1 (1.46e-3) +	1.9153e-1 (9.87e-4)	1.9091e-1 (9.84e-4) ≈
	10	2.8037e-1 (4.33e-3) —	4.7354e-1 (2.22e-2) —	3.1670e-1 (1.02e-2) —	4.2251e-1 (3.81e-2) —	2.1641e-1 (1.86e-3) +	2.3088e-1 (1.90e-3)	2.2966e-1 (1.40e-3) +
	15	3.2349e-1 (7.07e-3) —	5.3343e-1 (2.66e-2) —	3.3722e-1 (1.52e-2) —	5.1403e-1 (1.96e-2) —	2.8147e-1 (2.86e-3) +	3.0765e-1 (3.17e-3)	3.0757e-1 (2.94e-3) ≈
	20	4.4722e-1 (1.62e-2) —	6.3921e-1 (3.24e-2) —	4.5538e-1 (9.15e-3) —	6.3078e-1 (4.82e-2) —	3.4677e-1 (3.15e-3) +	3.9486e-1 (3.50e-3)	3.7910e-1 (4.12e-3) +
MaF2	5	1.1179e-1 (2.58e-3) —	1.3317e-1 (3.48e-3) —	1.2348e-1 (1.82e-3) —	8.1809e-2 (2.03e-3) +	9.4529e-2 (1.77e-3) +	9.6874e-2 (2.32e-3)	9.6708e-2 (1.83e-3) ≈
	8	1.8030e-1 (2.74e-2) —	2.1154e-1 (5.33e-2) —	1.6225e-1 (7.23e-3) —	4.3397e-1 (3.56e-2) —	1.7974e-1 (1.20e-2)	1.5138e-1 (3.69e-3)	1.4937e-1 (4.89e-3) ≈
	10	2.1362e-1 (2.38e-2) —	2.8261e-1 (3.51e-2) —	1.9919e-1 (7.44e-2) —	5.0525e-1 (2.38e-2) —	2.2553e-1 (1.85e-2) —	1.8049e-1 (8.58e-3)	1.8745e-1 (6.99e-3) —
	15	2.3128e-1 (2.68e-2) —	4.1832e-1 (4.23e-2) —	2.8506e-1 (2.10e-2) —	6.1326e-1 (3.18e-2) —	3.5296e-1 (3.30e-2) —	2.0940e-1 (7.50e-3)	3.3823e-1 (3.61e-2) —
	20	4.5707e-1 (6.91e-2) —	7.8626e-1 (2.38e-2) —	6.6574e-1 (4.79e-2) —	3.4395e-1 (1.76e-2) —	2.0129e-1 (8.37e-3) —	4.3639e-1 (2.32e-2)	4.3639e-1 (2.32e-2)
MaF3	5	2.3212e+1 (2.84e+1) —	6.4527e+1 (5.05e+1) —	3.3207e+0 (3.98e+0) —	1.9522e+0 (1.88e+0) —	4.1656e-1 (5.47e-1) ≈	4.1367e-1 (6.16e-1)	4.4466e-1 (6.94e-1) ≈
	8	1.1890e+2 (2.00e+2) —	1.6228e+2 (1.11e+2) —	1.4371e+1 (1.30e+1) ≈	1.2246e+2 (1.66e+2) —	4.6944e-1 (9.95e-1) +	2.2936e+1 (4.87e+1)	2.0736e+1 (4.82e+1) +
	10	8.8843e+3 (2.82e+4) ≈	2.0891e+2 (1.93e+2) —	3.5934e+1 (6.66e+1) +	1.7573e+2 (1.42e+2) +	1.4302e-1 (8.75e-3) +	3.4255e+3 (6.54e+3)	2.2294e+3 (2.67e+3) ≈
	15	4.7463e+3 (7.31e+3) —	2.6389e+2 (2.37e+2) —	1.1165e+2 (9.93e+1) —	2.1761e+2 (1.77e+2) —	1.7275e-1 (1.20e-1) +	3.8565e+0 (4.82e+0)	5.9408e+3 (7.84e+3) ≈
	20	4.1921e+3 (1.05e+6) —	3.1322e+2 (2.72e+2) —	1.2664e+3 (2.27e+3) +	2.0258e-1 (8.07e-1) +	4.7584e-1 (8.07e-1) +	9.0965e+3 (1.13e+4)	8.3636e+3 (1.44e+4) ≈
MaF4	5	1.3645e+1 (1.50e+1) —	6.8358e+0 (5.80e+0) —	3.7499e+0 (2.84e+0) —	7.7731e+0 (1.06e+0) —	3.6128e+0 (3.14e+0) —	2.6931e+0 (2.22e+0)	2.6335e+0 (1.23e+0) +
	8	1.0721e+2 (1.06e+2) —	6.9810e+1 (7.77e+0) —	2.8857e+1 (3.77e+0) —	7.2767e+1 (1.15e+1) —	4.6763e+1 (9.22e+0) —	1.5935e+1 (1.29e+0) +	1.7909e+1 (1.92e+0) —
	10	2.0749e+2 (2.05e+2) —	3.9683e+2 (1.90e+1) —	1.0885e+2 (9.20e+0) —	2.9580e+2 (3.28e+1) —	1.8730e+2 (4.75e+1) —	6.0441e+1 (5.12e+0)	6.3521e+1 (5.39e+0) ≈
	15	6.3557e+3 (8.14e+3) —	1.4154e+4 (3.22e+3) —	4.9375e+3 (3.19e+3) —	1.0210e+4 (1.94e+3) —	7.1462e+3 (1.38e+3) —	2.8850e+3 (3.98e+3)	1.7680e+3 (3.01e+2) ≈
	20	4.2975e+5 (4.04e+5) —	4.1936e+5 (1.05e+5) —	1.6926e+5 (1.02e+5) —	2.4579e+5 (7.01e+4) —	6.7886e+4 (3.48e+4)	6.2136e+4 (4.20e+4) ≈	
MaF5	5	1.9711e+0 (8.31e-3) —	3.9949e+0 (1.99e-1) —	1.9647e+0 (6.57e-3) —	3.7785e+0 (3.73e-1) —	1.3258e+1 (2.37e+0) —	1.9158e+0 (6.08e-2) —	3.2065e+0 (3.27e-1) —
	8	1.7021e+1 (4.44e-1) +	7.3943e+1 (3.56e+0) —	1.7434e+1 (4.64e-1) +	4.9016e+1 (4.07e+0) —	7.2767e+1 (1.15e+1) —	4.6763e+1 (9.22e+0) —	3.0175e+1 (5.65e+0) —
	10	7.7927e+1 (1.49e+0) —	2.9012e+2 (9.63e+0) —	7.7474e+1 (1.79e+0) +	1.9988e+2 (1.59e+1) —	2.9764e+2 (3.06e+1) —	1.2722e+2 (2.32e+1)	1.7639e+2 (2.83e+1) —
	15	2.2606e+3 (1.50e+2) +	7.2911e+1 (4.19e+1) —	2.1563e+3 (2.06e+2) +	6.0855e+3 (1.22e+2) —	7.1049e+3 (7.12e+2) —	5.0865e+3 (9.37e+2)	5.9062e+3 (4.50e+2) —
	20	7.0786e+4 (1.40e+4) —	1.7076e+5 (4.23e+2) —	6.9717e+5 (3.22e+2) —	1.4336e+5 (2.28e+3) —	1.6947e+5 (6.06e+3) —	1.3258e+5 (1.74e+4)	1.3995e+5 (3.18e+3) —
MaF6	5	1.5499e-2 (2.62e-2) —	6.0162e-2 (7.95e-3) —	7.7475e-2 (1.35e-2) —	2.1202e-3 (3.22e-5) +	1.0089e-2 (2.47e-3) —	3.2341e-3 (3.24e-4) —	2.8386e-3 (2.33e-4) +
	8	2.5535e-1 (3.96e-1) —	8.6216e-2 (1.86e-2) —	1.2310e-1 (1.77e-1) —	1.8495e-3 (3.35e-5) —	1.4938e-2 (8.56e-3) —	2.8202e-3 (2.24e-4)	5.3145e-2 (2.19e-1) —
	10	9.2931e-1 (3.21e-1) —	9.7635e-2 (2.22e-2) —	2.4669e-1 (3.59e-1) —	1.6007e-3 (1.94e-5) —	8.3694e-3 (3.29e-3) —	2.0626e-1 (4.37e-1)	2.1303e-1 (2.97e-1) —
	15	1.9607e+0 (1.38e+0) ≈	1.5181e-1 (2.42e-1) —	1.0098e+0 (5.93e+0) ≈	2.5439e-3 (7.29e-5) —	4.5590e-3 (5.47e-4) —	1.1655e+0 (5.25e-1)	1.1141e+0 (4.99e-1) ≈
	20	8.1939e+0 (8.75e+0) —	1.2653e-1 (8.36e-2) —	1.8556e+0 (1.16e+0) ≈	4.0188e-3 (1.99e-4) —	5.0408e-3 (6.65e-4) —	1.3629e+0 (5.25e-1)	1.0832e+0 (5.18e-1) ≈
MaF7	5	5.1882e-1 (1.13e-2) —	2.8730e+0 (5.70e-1) —	2.9968e-1 (1.80e-2) —	3.1971e-1 (2.96e-2) —	3.2043e-1 (3.64e-2) —	2.7164e-1 (5.97e-2) —	2.6210e-1 (8.61e-2) +
	8	7.3546e-1 (5.22e-2) —	1.7031e+0 (4.13e-1) —	7.83532e-1 (2.63e-1) —	1.2055e+0 (2.44e-1) —	8.4023e-1 (2.65e-2) —	5.5952e-1 (2.18e-2)	5.4541e-1 (6.98e-3) +
	10	1.5248e+0 (2.42e-1) —	1.9670e+0 (3.02e-1) —	8.9265e-1 (8.06e-2) ≈	2.1830e+0 (4.81e-1) —	1.5412e+0 (2.48e-1) —	9.1987e-1 (2.67e-2)	8.4336e-1 (1.42e-2) +
	15	7.3350e+0 (1.72e+0) —	3.3810e+0 (7.84e-2) —	3.7711e+0 (7.59e-1) —	2.9534e+0 (2.97e-1) —	4.3780e+0 (1.04e+0) —	2.1084e+0 (1.44e-1)	1.7967e+0 (1.97e-1) —
	20	1.0845e+1 (1.16e+0) —	1.5942e+1 (4.59e-1) —	9.7018e+0 (1.27e+0) —	4.0361e+0 (4.88e-1) —	6.7232e+0 (8.12e-1) —	5.5559e+0 (9.03e-1)	2.0609e+0 (8.62e-2) +
MaF8	5	1.7856e-1 (3.31e-2) —	3.0612e-1 (3.52e-2) —	3.2809e-1 (5.14e-2) —	3.9677e-1 (7.07e-2) —	9.4017e-2 (3.62e-2) —	8.6250e-2 (1.85e-2)	8.2067e-2 (2.17e-2) +
	8	2.9017e-1 (4.19e-2) —	5.6769e-1 (3.85e-2) —	5.59545e-1 (6.09e-2) —	3.9082e-1 (6.11e-2) —	1.3314e-1 (2.95e-3) —	1.0189e-1 (5.04e-3)	1.1465e-1 (1.52e-2) —
	10	10.2172e-1 (4.89e-2) —	8.2038e-1 (2.78e-1) —	7.2035e-1 (1.60e-1) —	3.7965e-1 (5.74e-2) —	1.4385e-1 (1.22e-2) —	1.0381e-1 (2.45e-1) —	1.4051e-1 (3.26e-3) —
	15	3.5817e-1 (6.36e-2) —	1.1022e+0 (2.04e-1) —	9.3656e-1 (1.34e-1) —	2.9774e-1 (6.44e-2) —	1.9045e-1 (1.29e-2) —	1.4420e-1 (2.19e-2)	2.0589e-1 (2.27e-2) —
	20	4.2641e-1 (7.08e-2) —	1.6617e+0 (2.75e-1) —	9.4765e-1 (1.99e-1) —	3.0174e-1 (5.69e-2) —	2.4817e-1 (1.95e-2) —	1.9199e-1 (2.43e-2)	2.2438e-1 (1.64e-2) —
MaF9	5	3.3034e-1 (1.36e-1) —	2.3980e-1 (2.15e-2) —	7.0529e-1 (3.19e-1) —	2.1853e-1 (3.49e-2) —	1.3605e-1 (4.61e-3) —	7.7703e-2 (8.69e-3) —	7.6803e-2 (7.63e-3) ≈
	8	2.9017e-1 (4.19e-2) —	5.6769e-1 (3.85e-2) —	5.59545e-1 (6.09e-2) —	3.9082e-1 (6.11e-2) —	1.3314e-1 (2.95e-3) —	1.0189e-1 (5.04e-3)	1.1465e-1 (1.52e-2) —
	10	10.2172e-1 (4.89e-2) —	8.2038e-1 (2.78e-1) —	7.2035e-1 (1.60e-1) —	3.7965e-1 (5.74e-2) —	1.4385e-1 (1.22e-2) —	1.0381e-1 (2.45e-1) —	1.4051e-1 (3.26e-3) —
	15	3.5817e-1 (6.36e-2) —	1.1022e+0 (2.04e-1) —	9.3656e-1 (1.34e-1) —	2.9774e-1 (6.44e-2) —	1.9045e-1 (1.29e-2) —	1.4420e-1 (2.19e-2)	2.0589e-1 (2.27e-2) —
	20	4.2641e-1 (7.08e-2) —	1.6617e+0 (2.75e-1) —	9.4765e-1 (1.99e-1) —	3.0174e-1 (5.69e-2) —	2.4817e-1 (1.95e-2) —	1.9199e-1 (2.43e-2)	2.2438e-1 (1.64e-2) —
MaF10	5	1.1805e+0 (9.06e-2) ≈	1.4434e+0 (1.94e-1) —	8.8973e-1 (8.68e-2) +	1.0642e+0 (8.93e-2) +	8.0165e-1 (8.29e-2) +	1.1140e+0 (1.42e-1)	9.0474e-1 (1.119e-1) +
	8	1.9620e+0 (1.31e-1) —	2.2886e+0 (1.90e-1) —	1.3824e+0 (1.52e-1) —	1.8561e+0 (7.31e-2) —	1.4518e+0 (1.12e-1) +	1.6522e+0 (1.31e-1)	1.5933e+0 (1.12e-1) ≈
	10	2.1390e+0 (1.57e-1) —	1.9463e+0 (1.29e-1) —	1.4304e+0 (1.42e-1) —	2.1138e+0 (1.81e-1) —	1.6100e+0 (8.89e-2) —	1.7727e+0 (1.77e-2)	1.7117e+0 (7.85e-2) ≈
	15	2.8006e+0 (1.82e-1) —	3.1252e+0 (2.32e-1) —	1.9300e+0 (7.87e-2) +	3.0347e+0 (1.54e-1) —	2.2023e+0 (6.80e-2) —	2.1831e+0 (1.62e-1)	2.1177e+0 (1.86e-1) ≈
	20	2.4774e+0 (1.99e-1) —	4.0776e+0 (1.29e-1) —	4.0364e+0 (2.22e-1) —	4.8146e+0 (1.48e-1) —	5.0147e+0 (1.10e-1) —	3.8758e+0 (3.04e-1)	3.6598e+0 (2.44e-1) +
MaF11	5	8.8737e-1 (2.58e-3) +	4.7620e-2 (1.74e-3) —	3.8784e-1 (4.01e-3) —	5.6828e-1 (5.43e-2) —	4.9259e-1 (3.78e-2) —	4.3701e-1 (1.45e-1) —	6.7300e-1 (1.53e-1) —
	8	9.1129e+0 (1.129e-1) +	1.1396e+0 (6.29e-2) +	5.6097e-1 (7.87e-2) —	1.9522e-1 (3.37e-2) —	1.6842e-1 (1.36e-2) —	1.3206e+0 (1.15e-1) ≈	1.3136e+0 (1.22e-1) —
	10	1.2047e+0 (1.47e-1) +	1.2842e+0 (3.95e-2) +	1.1477e+0 (7.93e-2) +	1.7462e+0 (7.78e-2) —	1.6732e+0 (1.30e-1) —	1.4424e+0 (9.58e-2)	1.9149e+0 (9.95e-2) —
	15	1.5497e+0 (5.83e-2) +	1.9420e+0 (7.52e-2) +	3.9004e+0 (1.43e-0) —	2.2131e+0 (7.56e-2) —	2.3300e+0 (8.10e-2) —	2.0971e+0 (8.77e-2)	2.4567e+0 (6.74e-2) —
	20	3.9033e+0 (2.23e-1) +	5.4337e+0 (7.59e-2) +	4.6766e+0 (1.00e-0) —	4.7089e+0 (1.81e-1) —	5.1649e+0 (1.12e-1) —	4.2077e+0 (2.73e-1)	5.0068e+0 (2.01e-1) —
MaF12	5	9.3516e-1 (4.12e-3) —	1.0397e+0 (8.22e-3) —	9.2648e-1 (3.12e-3) ≈	1.3789e+0 (2.12e-1) —	9.7306e-1 (1.20e-2) —	9.2982e-1 (6.46e-3) —	9.4253e-1 (1.35e-2) —
	8	2.8156e+0 (4.02e-2) —	3.2324e+0 (3.83e-2) —	2.7773e+0 (1.58e-2) —	3.7436e+0 (1.79e-2) —	2.8866e+0 (2.22e-2) —	2.7572e+0 (1.96e-2) —	2.7361e+0 (1.61e-2) +
	10	4.3314e+0 (3.82e-2) —	5.2400e+0 (3.35e-1) —	4.2973e+0 (4.24e-2) —	5.4504e+0 (2.22e-2) —	4.2707e+0 (4.67e-2) —	3.9734e+0 (2.91e-2) —	4.0360e+0 (2.75e-2) —

TABLE S-XII
HV RESULTS OF ALL METHODS ON MAF1–MAF15 WITH $G_{\max}=200$.

Problem	M	NSGA-III	MOEA/DD	θ -DEA	Iby1EA	NSGA-II/SDR	MultiGPO	MultiGPO2
MaF1	5	6.3765e-3 (3.80e-4) —	5.7992e-3 (5.80e-5) —	6.0146e-3 (4.11e-4) —	1.3199e-2 (2.05e-4) +	1.3017e-2 (1.27e-4) +	1.1477e-2 (2.67e-4) —	1.1912e-2 (2.30e-4)
	8	3.0700e-5 (1.83e-6) ≈	1.2188e-5 (2.19e-6) —	2.9017e-5 (1.41e-6) ≈	3.7482e-5 (1.32e-5) ≈	4.1304e-5 (2.68e-6) +	3.0951e-5 (6.70e-6) ≈	3.1990e-5 (6.37e-6)
	10	4.7264e-2 (2.67e-8) +	3.5240e-8 (1.07e-8) —	3.4518e-7 (4.13e-8) —	9.8517e-8 (4.76e-8) —	5.1304e-7 (2.28e-7) +	2.9285e-7 (5.62e-7) ≈	3.9951e-7 (6.80e-7)
	15	5.79e-12 (1.03e-12) +	2.23e-13 (7.60e-14) +	5.52e-12 (1.13e-13) +	3.45e-13 (1.12e-13) +	3.76e-10 (1.69e-9) ≈	0.00e+0 (0.00e+0) ≈	0.00e+0 (0.00e+0)
MaF2	5	1.8761e-1 (2.86e-3) ≈	1.5337e-1 (2.90e-3) —	1.7315e-1 (2.33e-3) —	1.8889e-1 (2.13e-3) ≈	2.0316e-1 (1.87e-3) +	1.8432e-1 (2.56e-3) —	1.8824e-1 (3.33e-3)
	8	2.1528e-1 (6.84e-3) —	1.5882e-1 (3.83e-3) —	1.8207e-1 (8.01e-3) —	2.1655e-1 (3.10e-3) —	2.3236e-1 (2.25e-3) +	2.2030e-1 (3.72e-3) —	2.2359e-1 (2.48e-3)
	10	2.1631e-1 (5.06e-3) —	1.7271e-1 (7.31e-3) —	1.9509e-1 (9.13e-3) —	1.4876e-1 (7.71e-3) —	2.2247e-1 (2.48e-3) —	2.1111e-1 (4.22e-3) —	2.2558e-1 (3.74e-3)
	15	1.3875e-1 (1.52e-2) —	9.3783e-2 (3.91e-3) —	1.2494e-1 (1.13e-2) —	1.4365e-1 (1.04e-2) —	2.0563e-1 (5.44e-3) —	1.6979e-1 (3.84e-3) —	2.1734e-1 (2.78e-3)
MaF3	5	1.0066e-1 (1.76e-2) —	1.4443e-1 (5.42e-3) —	1.6984e-1 (3.16e-3) —	1.3979e-1 (8.98e-3) —	2.1606e-1 (2.84e-3) ≈	1.4941e-1 (5.32e-3) —	2.1585e-1 (3.08e-3)
	8	1.3362e-2 (5.98e-2) —	0.00e+0 (0.00e+0) —	3.0279e-1 (4.38e-1) —	3.2090e-1 (4.44e-1) —	7.5155e-1 (3.91e-1) —	7.7892e-1 (3.62e-1) ≈	8.0438e-1 (3.06e-1)
	10	5.9982e-1 (5.07e-1) ≈	6.6580e-1 (4.30e-1) —	9.9717e-1 (1.86e-3) —	9.9906e-1 (4.79e-4) —	9.9213e-1 (1.75e-3) —	9.9996e-1 (4.23e-5) +	9.9886e-1 (1.29e-3)
	15	0.00e+0 (0.00e+0) ≈	6.3930e-2 (1.94e-1) +	0.00e+0 (0.00e+0) ≈	9.9362e-1 (2.48e-3) +	0.00e+0 (0.00e+0) ≈	0.00e+0 (0.00e+0) ≈	0.00e+0 (0.00e+0)
MaF4	5	1.0203e-2 (1.76e-2) —	1.9401e-2 (1.79e-2) —	6.2437e-2 (2.94e-2) —	3.0588e-2 (1.47e-2) —	8.2040e-2 (4.20e-2) ≈	8.5938e-2 (3.22e-2) ≈	8.8647e-2 (2.84e-2)
	8	1.9658e-3 (1.92e-4) —	2.4531e-5 (1.23e-5) —	1.1795e-3 (3.53e-4) —	1.9503e-4 (9.68e-5) —	7.0521e-4 (1.70e-4) —	7.1516e-3 (2.53e-4) +	2.0274e-3 (1.83e-4)
	10	2.8831e-5 (4.27e-5) —	1.4586e-7 (9.65e-8) —	1.9771e-4 (3.06e-5) +	1.6273e-6 (1.63e-6) —	1.3139e-5 (8.56e-6) —	7.6165e-5 (3.05e-5) ≈	6.1068e-5 (2.07e-5)
	15	1.826e-8 (2.80e-13) —	1.175e-8 (9.63e-8) —	7.686e-10 (1.52e-10) —	1.436e-10 (1.52e-10) —	5.060e-9 (1.00e-8) ≈	5.049e-9 (1.08e-8)	
MaF5	5	8.0859e-1 (7.83e-4) —	6.8134e-1 (3.95e-3) —	8.1074e-1 (4.13e-4) +	6.7344e-1 (1.38e-2) —	1.8612e-1 (8.67e-2) —	8.0276e-1 (1.69e-3) +	7.6524e-1 (9.59e-3)
	8	9.2465e-1 (5.21e-4) +	5.8238e-1 (4.83e-2) —	9.2603e-1 (2.95e-4) —	7.0405e-1 (1.59e-2) —	1.1186e-1 (3.64e-2) —	8.8610e-1 (6.04e-3) ≈	8.8226e-1 (8.76e-3)
	10	9.6585e-1 (9.05e-4) —	5.7725e-1 (2.29e-2) —	9.6964e-1 (3.85e-4) —	7.9471e-1 (1.23e-2) —	1.0912e-1 (4.65e-2) —	9.2411e-1 (8.01e-3) +	9.1109e-1 (5.13e-3)
	15	9.8937e-1 (5.20e-4) +	4.6443e-1 (3.52e-2) —	9.9120e-1 (2.16e-4) +	8.2500e-1 (1.68e-2) —	1.1643e-1 (5.66e-2) —	9.7534e-1 (2.09e-3) +	9.4441e-1 (5.70e-3)
MaF6	5	9.9491e-1 (5.45e-3) +	4.8458e-1 (5.01e-2) —	9.9861e-1 (3.63e-5) +	8.4758e-1 (3.50e-2) —	1.0159e-1 (3.38e-3) —	9.8586e-1 (1.13e-3) +	9.6654e-1 (2.76e-3)
	8	1.2355e-1 (1.38e-3) —	1.0189e-1 (7.23e-3) —	1.1651e-1 (1.21e-3) —	1.2985e-1 (3.73e-4) +	1.2542e-1 (1.50e-3) —	1.2995e-1 (3.45e-4) +	1.2924e-1 (3.42e-4)
	10	8.8085e-2 (3.04e-2) —	9.6397e-2 (6.69e-4) —	1.0297e-1 (9.38e-4) —	1.0641e-1 (3.14e-4) —	1.0379e-1 (1.35e-3) —	1.0609e-1 (3.02e-4) +	1.0536e-1 (3.28e-4)
	15	2.01e-15 (9.02e-15) —	8.7778e-2 (7.67e-3) ≈	7.1880e-2 (4.26e-2) ≈	1.0103e-1 (3.13e-4) —	9.9420e-2 (3.97e-4) ≈	7.5407e-2 (4.47e-2) +	6.4905e-2 (4.89e-2)
MaF7	5	0.00e+0 (0.00e+0) ≈	8.7349e-2 (6.36e-3) +	4.6164e-4 (2.06e-3) —	9.5204e-2 (2.44e-4) +	9.4923e-2 (3.35e-4) +	0.00e+0 (0.00e+0) ≈	0.00e+0 (0.00e+0)
	8	8.7957e-2 (3.93e-3) —	0.00e+0 (0.00e+0) ≈	9.3235e-2 (3.47e-4) —	9.3218e-2 (3.05e-4) —	0.00e+0 (0.00e+0) ≈	0.00e+0 (0.00e+0) ≈	0.00e+0 (0.00e+0)
	10	2.4617e-1 (4.94e-3) —	9.4934e-2 (1.80e-2) —	2.1755e-1 (9.00e-3) —	1.8745e-1 (1.99e-2) —	2.5629e-1 (1.92e-3) —	2.4488e-1 (3.39e-3) —	2.6235e-1 (5.80e-3)
	15	2.0682e-1 (2.50e-3) +	3.1157e-2 (2.69e-2) —	1.8497e-1 (2.20e-2) +	8.4737e-2 (1.43e-2) —	2.0215e-1 (4.55e-3) +	1.3835e-1 (1.54e-2) ≈	1.3665e-1 (2.83e-2)
MaF8	5	1.4455e-1 (9.08e-3) —	1.0576e-4 (8.76e-5) —	1.5901e-1 (1.25e-2) +	9.4046e-2 (1.41e-2) —	1.5614e-1 (2.70e-2) —	9.7545e-2 (2.05e-2) —	1.0896e-1 (2.61e-2)
	8	3.4615e-2 (1.55e-2) —	6.2965e-7 (2.26e-7) —	8.2969e-2 (1.69e-2) —	4.7447e-5 (1.21e-4) —	7.2789e-2 (3.82e-2) ≈	7.0227e-2 (1.99e-2) —	8.4823e-2 (1.78e-2)
	10	1.0396e-1 (1.17e-2) +	0.00e+0 (0.00e+0) —	1.3336e-1 (7.24e-3) +	7.6404e-10 (1.80e-9) —	0.00e+0 (0.00e+0) —	7.8664e-2 (2.12e-2) +	2.3062e-2 (1.62e-2)
	15	1.0452e-1 (8.52e-3) —	8.2569e-2 (5.78e-3) —	7.7621e-2 (1.14e-2) —	9.8281e-2 (7.45e-3) —	1.2398e-1 (4.36e-4) —	1.2440e-1 (3.57e-3) —	1.2547e-1 (1.89e-3)
MaF9	5	2.6453e-2 (7.80e-4) —	1.8871e-2 (1.71e-3) —	1.7385e-2 (2.79e-3) —	2.9923e-2 (9.70e-4) —	3.1411e-2 (1.74e-4) —	3.1803e-2 (2.30e-4) —	3.2087e-2 (9.81e-5)
	8	9.0671e-3 (8.10e-4) —	6.1590e-3 (4.45e-4) —	5.6380e-3 (1.13e-3) —	1.0856e-2 (2.06e-4) —	1.0937e-2 (8.02e-5) —	1.1038e-2 (9.38e-5) —	1.1205e-2 (1.01e-4)
	10	4.7765e-4 (5.96e-5) —	3.2985e-4 (6.32e-5) —	2.8673e-4 (5.79e-5) —	6.4477e-4 (2.65e-5) ≈	6.2364e-4 (1.14e-5) —	6.1519e-4 (2.91e-5) —	6.4627e-4 (3.50e-5)
	15	2.2149e-5 (6.47e-6) —	1.2895e-5 (2.91e-6) —	1.5270e-5 (2.96e-6) —	3.6670e-5 (2.24e-6) —	3.5435e-5 (2.32e-6) —	3.5646e-5 (4.15e-6) —	3.9087e-5 (3.32e-6)
MaF10	5	2.2187e-1 (4.30e-2) —	2.4549e-1 (9.44e-3) —	1.3514e-1 (6.14e-2) —	2.4691e-1 (1.48e-2) —	2.8975e-1 (2.47e-3) —	3.2198e-1 (4.25e-3) ≈	3.2234e-1 (3.88e-3)
	8	2.2327e-2 (1.33e-2) —	2.2812e-2 (3.45e-3) —	2.3232e-2 (1.16e-2) —	5.1313e-2 (7.38e-4) —	4.5157e-2 (6.21e-4) —	5.2864e-2 (2.31e-4) —	5.3019e-2 (1.71e-4)
	10	9.1494e-3 (2.03e-3) —	8.4519e-3 (1.72e-3) —	5.8888e-3 (1.00e-3) —	1.8555e-3 (1.93e-4) —	1.6124e-2 (2.01e-4) —	1.8756e-2 (2.03e-4) ≈	1.8741e-2 (1.72e-4)
	15	6.5996e-4 (3.64e-4) —	6.1558e-4 (1.51e-4) —	4.0449e-4 (1.71e-4) —	1.3185e-3 (6.54e-5) +	1.1340e-3 (5.10e-5) —	1.1858e-3 (3.14e-4) —	1.1879e-3 (2.81e-4)
MaF11	5	2.4769e-6 (5.10e-6) —	1.1916e-5 (1.20e-5) —	4.7790e-6 (9.72e-6) —	2.8036e-5 (2.89e-5) —	4.3923e-5 (2.18e-5) —	3.1010e-5 (3.15e-5) —	4.7666e-5 (2.56e-5)
	8	7.7143e-1 (4.11e-2) —	6.4499e-1 (7.72e-2) —	9.3153e-1 (4.46e-2) —	9.8116e-1 (2.23e-2) —	9.8810e-1 (9.70e-3) —	8.7062e-1 (5.27e-2) —	9.9786e-1 (5.52e-4)
	10	4.3520e-1 (5.20e-2) —	4.7966e-1 (5.74e-2) —	7.0815e-1 (3.97e-2) —	4.7075e-1 (4.17e-2) —	7.5147e-1 (4.12e-2) —	5.2924e-1 (7.24e-2) —	8.5714e-1 (6.52e-2)
	15	4.4165e-2 (1.65e-2) —	3.4889e-1 (5.81e-2) —	8.6738e-1 (7.13e-2) —	3.8976e-1 (3.81e-2) —	8.9638e-1 (6.91e-2) —	6.7555e-1 (7.69e-2) —	9.2525e-1 (7.08e-2)
MaF12	5	9.6723e-1 (1.53e-2) —	6.3764e-1 (1.72e-2) —	6.3678e-1 (1.53e-2) —	9.3055e-1 (2.18e-2) —	9.3055e-1 (2.18e-2) —	7.4909e-1 (8.37e-2) —	9.6776e-1 (5.28e-2)
	8	9.9312e-1 (2.78e-3) +	9.6798e-1 (8.19e-3) —	9.9033e-1 (2.37e-3) —	9.9090e-1 (2.66e-3) —	9.7963e-1 (5.29e-3) —	9.9110e-1 (2.10e-3) —	9.9054e-1 (2.19e-3)
	10	9.9047e-1 (5.65e-3) +	9.5596e-1 (7.54e-3) —	9.8441e-1 (4.62e-3) —	9.8217e-1 (3.34e-3) —	9.8184e-1 (3.89e-3) —	9.8604e-1 (2.33e-3) +	9.8391e-1 (2.71e-3)
	15	9.8708e-1 (4.29e-3) —	9.6186e-1 (1.03e-3) —	9.0847e-1 (6.51e-2) —	9.8081e-1 (4.92e-3) —	9.8623e-1 (3.71e-3) —	9.8956e-1 (2.68e-3) —	9.8955e-1 (4.27e-3)
MaF13	5	9.6273e-1 (3.42e-2) —	9.5424e-1 (1.98e-2) —	9.5424e-1 (1.78e-2) —	9.7802e-1 (6.70e-3) —	9.8609e-1 (4.84e-3) —	9.9087e-1 (3.36e-3) —	9.9289e-1 (3.04e-3)
	8	7.7494e-1 (5.18e-2) —	7.0533e-2 (7.89e-3) —	8.2707e-1 (3.37e-2) —	7.1752e-1 (3.99e-2) —	8.0378e-1 (7.46e-3) +	8.5401e-1 (5.09e-3)	
	10	8.0337e-1 (5.67e-2) —	6.1236e-1 (5.43e-2) —	8.3888e-1 (1.17e-2) —	7.2315e-1 (2.06e-2) —	8.8661e-1 (3.87e-2) +	8.1698e-1 (1.37e-2) —	8.6481e-1 (3.68e-2)
	15	7.9890e-1 (4.17e-2) —	5.6639e-1 (8.74e-2) —	7.8417e-1 (4.16e-2) —	7.0220e-1 (4.32e-2) —	9.0608e-1 (3.79e-2) +	7.9324e-1 (1.53e-2) —	8.6585e-1 (4.20e-2)
MaF14	5	2.2505e-1 (2.07e-2) —	2.1735e-1 (3.86e-2) —	1.3550e-1 (4.29e-2) —	2.8192e-1 (6.27e-3) +	2.4026e-1 (9.83e-3) —	2.6729e-1 (1.32e-2) —	2.6073e-1 (1.13e-2)
	8	1.2007e-1 (1.82e-2) —	7.0533e-2 (7.89e-3) —	1.3072e-1 (2.17e-2) —	1.8072e-1 (1.70e-3) —	1.4809e-1 (5.54e-3) —	1.6577e-1 (6.33e-3) —	1.6159e-1 (5.30e-3)
	10	9.4218e-2 (2.47e-2) —	4.5940e-2 (1.67e-2) —	3.0399e-2 (3.42e-3) —	1.4213e-1 (2.03e-3) —	1.1191e-1 (6.10e-3) —	1.2439e-1 (1.19e-2) —	1.3093e-1 (2.88e-3)
	15	5.5112e-2 (1.74e-2) —	3.2986e-2 (1.35e-2) —	6.5019e-5 (1.20e-4) —	8.9864e-2 (1.77e-3) —	7.2776e-2 (3.47e-3) —	8.5869e-2 (5.62e-3) —	8.6709e-2 (1.48e-3)
MaF15	5	0.00e+0 (0.00e+0) —	1.3335e-3 (5.85e-3) —	0.00e+0 (0.00e+0) —	1.1415e-1 (9.11e-2) —	7.7150e-2 (6.94e-2) —	3.4695e-1 (6.32e-2) —	3.5297e-1 (8.09e-2)
	8	0.00e+0 (0.00e+0) —	6.4625e-2 (8.61e-2) —	0.00e+0 (0.00e+0) —	1.7153e-1 (1.02e-1) —	1.6346e-1 (1.27e-1) —	2.4210e-1 (1.75e-1) —	3.4002e-1 (1.93e-1)
	10	0.00e+0 (0.00e+0) —	0.00e+0 (0.00e+0) —	0.				